

EET 87503 and EET 87513

Paired Howardites, 1734.5 g and 394.5 g
Antarctic Finds

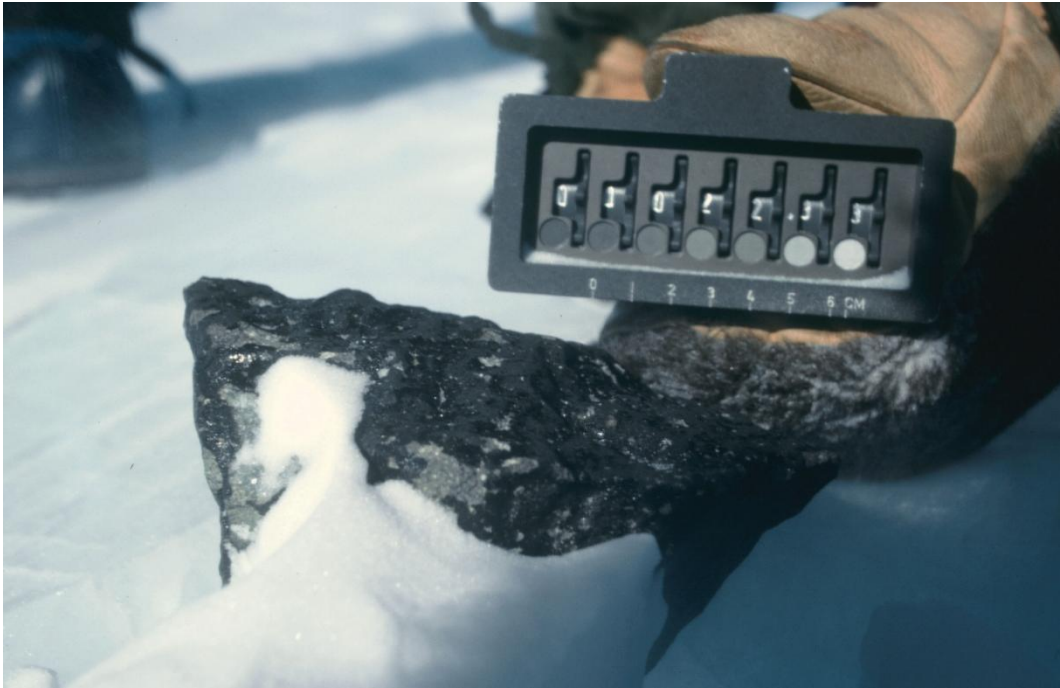


Figure 1: The EET 87503 howardite, as found in the Elephant Moraine ice field in the Transantarctic Mtns. Divisions at bottom of counter are 1 cm.

Introduction: The EET 87503 and EET 87513 meteorites (**Figures 1 and 2**) were collected in the Texas Bowl icefield of the Elephant Moraine collection field in Antarctica, during the 1987 ANSMET season (Antarctic Meteorite Newsletter, 11/2; Grossman, 1994; Buchanan et al, 2000). They were first reported in Volume 11, Issue 2 of the Antarctic Meteorite Newsletter published by the meteorite curation group at NASA-JSC, which noted their weights (87503: 1734.5 g, 87513: 394.5 g) and dimensions (87503: 16.5 cm x 10 cm x 8.5 cm; 87513: 11 cm x 6 cm x 4.5 cm), as well as their generally minimal terrestrial weathering effects (87503: A, 87513: A/B) and lack of fracturing (both meteorites are a category A). Both EET 87503 and EET 87513 have minor iron oxide staining, with the latter showing a slightly greater degree of alteration (Buchanan et al, 2000); however, geochemical data revealed that EET 87503 has also experienced an appreciable amount of alteration, especially in the outer portions of the stone (Mittlefehldt and Lindstrom, 1991a). Both meteorites have a glassy fusion crust, though it only partially covers EET 87503 while it completely encloses EET 87513 (Antarctic Meteorite Newsletter, 11/2).

EET 87503 and EET 87513 are classic howardites, displaying a variety of fine- to coarse-grained diogenite, eucrite (multiple varieties), impact melt/breccia, glassy, and even carbonaceous chondrite clasts in a light gray matrix (Antarctic Meteorite Newsletter, 11/2; Mittlefehldt and Lindstrom, 1991a; Buchanan et al, 2000; Buchanan, 2002). EET 87513 was originally investigated as part of two consortia between D. Mittlefehldt and M. Lindstrom at JSC, J.C. Laul at Pacific Northwest Laboratories, and A.M.

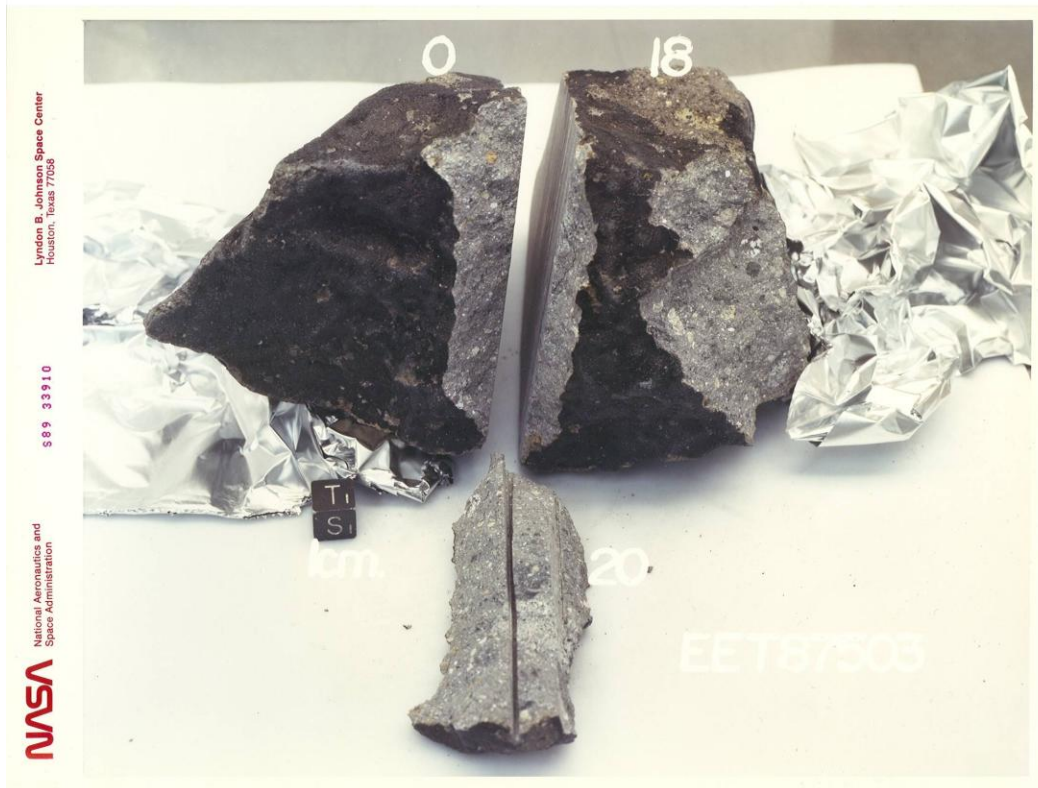


Figure 2a: The EET 87503 howardite, clearly showing both the external fusion crust and the internal light-gray matrix with varied clasts. Cube is 1 cm along each side. Photo courtesy of NASA-JSC (photo S89-33910).

Reid at the University of Houston; much of the early work on EET 87513 was done by P.C. Buchanan at the University of Houston for his Ph.D. dissertation (published in various reports cited herein, with the dissertation published in 1995).

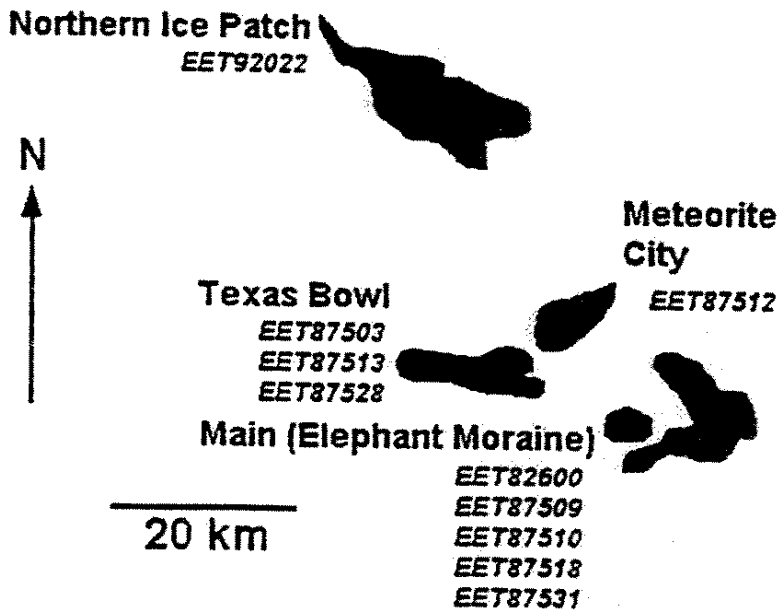
Part of the reason for these consortia was to discern actual pairings between a group of related meteorites; EET 87503 and EET 87513 were preliminarily paired with EET 87509, 87510, 87512, 87518, and 87531, both in the field and in early published reports (Antarctic Meteorite Newsletter, 11/2; Grossman, 1994). Various authors have proposed different pairings within the group (e.g., Sears et al, 1991 based on TL sensitivities and Mittlefehldt and Lindstrom, 1991a based on chemical analyses), and some have proposed that other meteorites found in the Elephant Moraine region may be related to the EET 87XXX group (e.g., EET 82600 and EET 92022: Mittlefehldt and Lindstrom, 1991a; Grossman and Score, 1996). A recent summary of possible pairings (Buchanan et al, 2000) suggests that EET 87503 and 87513 should be paired as more recently-fallen (less weathered) howardites, while EET 82600, 87509, 87510, 87518, and 87531 may be paired as polymict eucrites from an older fall, as they are more weathered and mostly lacking in the diogenite component seen in both EET 87503 and EET 87513. The same study suggested that EET 87512 and EET 92022 are probably unrelated to the other two groups (Buchanan et al, 2000). These pairings seem reasonable given that they are correlated to their collection locations within the Elephant Moraine (Buchanan et al, 2000; **Figure 3**).



Figure 2b: Pieces of the EET 87513 howardite, with varied clasts set in a light-gray matrix. Cubes have 1 cm sides. Photos courtesy of NASA-JSC.

Another howardite, EET 87528 (**Figure 4**), was also discovered in the Texas Bowl ice field in the same season, and was mentioned as a prospective pair with EET 87503 and EET 87513 (Sears et al, 1991; Buchanan et al, 2000); however, though it is similarly weathered and has similar overall composition, this meteorite has not been as thoroughly evaluated in the literature as the others, partly due to its small size (40.5 g), and thus it is mostly absent from this paper.

General Petrography: EET 87503 and EET 87513 generally consist of relatively large, mm- to cm-sized angular clastic fragments in a light gray, comminuted matrix (Antarctic Meteorite Newsletter, 11/2;



Buchanan and Mittlefehldt, 2003). Clasts are of many different varieties, including (1) fine-grained, deformed or brecciated, recrystallized orthopyroxenite clasts from diogenites, (2) equilibrated eucrite clasts, some with magnesian pyroxenes that approach diogenitic compositions and some with evolved

Figure 3: Map of Elephant Moraine collecting region in Antarctica; each specific field is

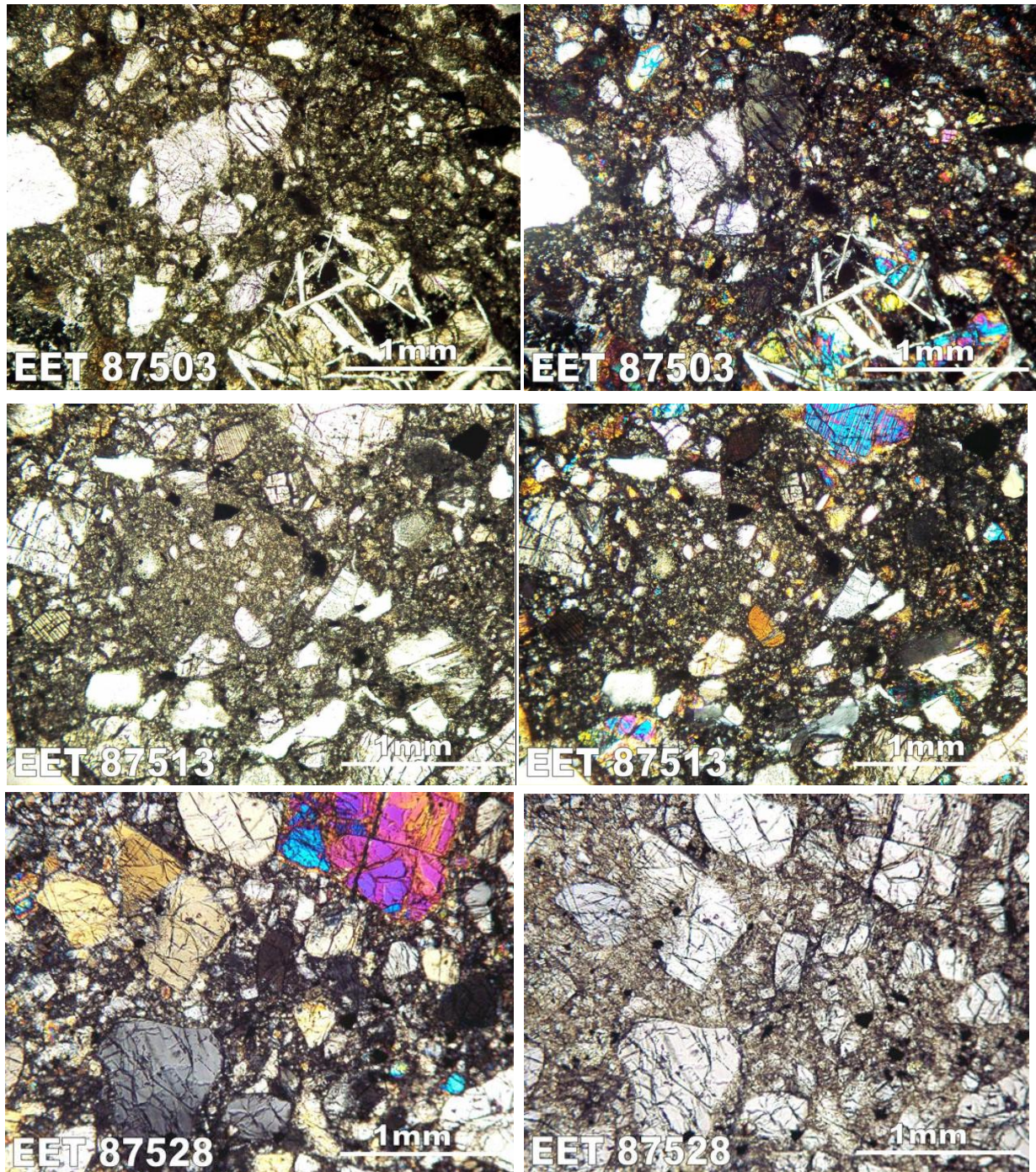
marked in black. Varied analyses of the EET87XXX meteorites (and others) suggest that each is paired with the others collected at the same locality. From Buchanan et al (2000).

melt compositions (i.e., Nuevo Laredo-type), (3) unequilibrated eucrite clasts with zoned pyroxene and plagioclase, (4) ≤ 2 cm aphanitic, black to brown, impact melt clasts and breccias, some of which are recrystallized, (5) lithified eucrite/howardite breccia clasts, and (6) at least one large (4 mm x 5 mm) and one small carbonaceous chondrite clast in EET87513, with Fukawa et al (2005) recently reporting that they isolated 26 carbonaceous clasts from the meteorite (Antarctic Meteorite Newsletter, 11/2; Mittlefehldt and Lindstrom, 1991a; Buchanan and Reid, 1991; Buchanan et al, 1990, 1993a, 1993b; Buchanan, 1995; Metzler et al, 1995; Buchanan et al, 2000; Buchanan and Lindstrom, 2000; Buchanan, 2002; Buchanan and Mittlefehldt, 2003). Eucrite clasts have textures that range from fine to coarse-grained, ophitic/subophitic to variolitic, vitrophyric, porphyritic, and brecciated, and their textural and compositional variety indicates that they were derived from cumulate, main-group, and evolved (i.e., Nuevo Laredo trend) eucrites (Mittlefehldt and Lindstrom, 1991a; Buchanan, 1995; Metzler et al, 1995; Buchanan et al, 2000; Buchanan and Lindstrom, 2000; Buchanan, 2002; Buchanan and Mittlefehldt, 2003).

Some pyroxenes show fine exsolution lamellae, and a number of clastic grains are strained, deformed, shocked, shock-blackened, recrystallized, or display mosaic or undulatory texture, though at least a few clasts are relatively unequilibrated and preserve primary igneous zoning in both pyroxene and plagioclase (Buchanan et al, 1990; Buchanan, 1995; Buchanan et al, 2000; Buchanan and Lindstrom, 2000; Buchanan, 2002; Buchanan and Mittlefehldt, 2003). Minerals in the eucrite/diogenite clasts include orthopyroxene, pigeonite, plagioclase, olivine, troilite, ilmenite, chromite, and cristobalite

(Antarctic Meteorite Newsletter, 11/2; Buchanan et al, 1990; Buchanan, 1995), with the carbonaceous chondrite material contributing olivine, orthopyroxene, and brown mesostasis (glassy or microcrystalline) in chondrules, and serpentine, saponite, pyrrhotite, pentlandite, enstatite, diopside, chromite, tochilinite, tochilinite-serpentine, carbonate grains, and carbonaceous spheres in the matrix (Zolensky et al, 1992; Buchanan et al, 1993a; Buchanan et al, 1993b).

Figure 4: Plane-polarized (left) and cross-polarized (right) thin section microphotographs of EET 87503, EET 87513, and EET 87528. From the NASA-JSC Antarctic Meteorite Curation website.



The light-gray matrix is composed of comminuted, submicroscopic to mm-sized pyroxene (both orthopyroxene and pigeonite) and plagioclase, with some larger mineral grains, rare ≤ 2.5 mm polymineralic clasts, and a small amount of opaques and other accessory minerals (Antarctic Meteorite Newsletter, 11/2; Buchanan and Mittlefehldt, 2003).

Lithic Clast and Matrix Petrography and Chemistry:

Author’s note: Because there is such a variety of mineral chemistries contained within the diverse lithic clasts, I have chosen to summarize compositions based on their host (lithic clast or matrix) rather than try to describe the wide range of mineral compositions without referencing where they were located in the meteorite. Each cited source contains further information for interested researchers. Some workers have reported clasts as sample numbers (e.g., 87503,23) and some have reported clast “names” (e.g., Clast A); I have tagged them as they are reported in the literature.

In addition, because many clasts are only briefly described over a limited number of sources, I apologize in advance to the original researchers if there is similar wording in a few cases, though I have tried to avoid it as best as possible. That being said, all original research and ideas are attributed directly to the sources that contain them.

EET 87503 Lithics: diogenites, eucrites, impact melt

Diogenites:

- Clast EET 87503,66 is a light-colored diogenitic orthopyroxenite with equigranular, cumulate pyroxene crystals ($\sim En_{70}$) up to 700 μm in diameter, with interstitial chromite (Metzler et al, 1995; **Figure 5**). REE patterns for this clast indicate LREE depletion relative to CI (Metzler et al, 1995; **Figure 6**). Bulk data is shown in **Table 1**, below.
- Clast D from EET 87503 is a deformed diogenite with undulatory extinction and mosaic texture (Buchanan and Lindstrom, 2000; Buchanan et al, 2002; Buchanan and Mittlefehldt, 2003).

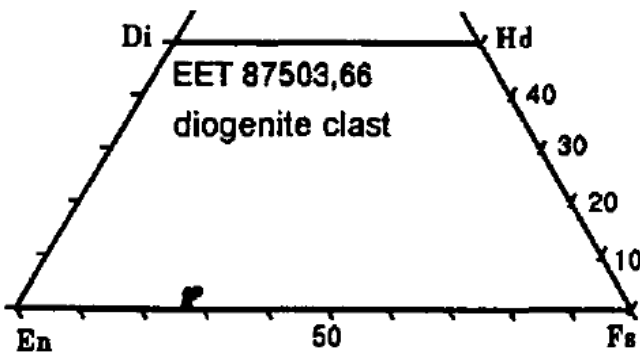


Figure 5: Pyroxene compositions from sample EET 87503,66, a diogenite clast. From Metzler et al (1995).

Figure 6: CI-normalized REE patterns for sample EET 87503,66, a diogenite clast, showing relative LREE depletion. From Metzler et al (1995).

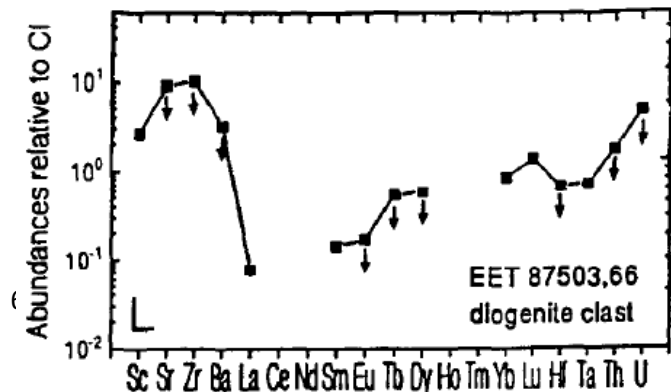


Table 1: Bulk INAA data for clast EET 87503,66, a recrystallized diogenite. From Metzler et al (1995).

reference	Metzler et al 95 EET 87503,66
weight	22.6 mg
wt% Ca	0.96
wt% Fe	12.78
Na ppm	125
K ppm	<5.00
Sc ppm	16.0
Cr ppm	3940
Mn ppm	4400
Co ppm	13.0
Ni ppm	45.0
Zn ppm	<15.0
Ga ppm	0.52
Se ppm	<0.25
Sr ppm	<80.0
Zr ppm	<40.0
Ba ppm	<7.00
La ppm	0.02
Sm ppm	<0.02
Eu ppm	<0.01
Tb ppm	<0.02
Dy ppm	<0.15
Yb ppm	0.14
Lu ppm	0.03
Hf ppm	<0.08
Ta ppm	<0.01
W ppm	<0.05
Ir ppm	<0.002
Au ppm	<0.001
Th ppm	<0.050
U ppm	<0.040
technique	INAA

Table 2: Bulk INAA data for fine-grained basalt clast EET 87503,62. From Metzler et al (1995).

reference	Metzler EET
weight	36.7 mg
wt% Ca	6.84
wt% Fe	15.8
Na ppm	4160
K ppm	520
Sc ppm	33.0
Cr ppm	2210
Mn ppm	4300
Co ppm	8.50
Ni ppm	25.00
Zn ppm	<45.0
Ga ppm	1.70
Se ppm	<0.40
Sr ppm	<70.0
Zr ppm	58.0
Ba ppm	49.0
La ppm	4.02
Ce ppm	10.8
Nd ppm	7.70
Sm ppm	2.56
Eu ppm	0.70
Gd ppm	3.70
Tb ppm	0.65
Dy ppm	4.21
Ho ppm	0.94
Tm ppm	0.39
Yb ppm	2.45
Lu ppm	0.36
Hf ppm	1.81
Ta ppm	0.25
W ppm	<0.15
Ir ppm	<0.002
Au ppm	<0.001
Th ppm	0.410
technique	INAA

Eucrites:

- Clasts EET 87503,23 and EET 87503,25 (fine-grained basalts) are evolved with respect to Juvinas-type eucrites; their compositions (Sc = 34-35 ppm, Sm = 2.2-2.5 ppm, FeO = 20-22 wt%) are similar to the evolved eucrite Lakagoan (Mittlefehldt and Lindstrom, 1991a). An interior sample of EET 87503,23 shows no evidence of REE transport due to terrestrial weathering, while the

exterior has slightly depleted LREE and a slight negative Ce anomaly (Mittlefehldt and Lindstrom, 2003).

- Clast EET 87503,53, a medium-grained basalt, shows no terrestrial weathering effects on an exterior sample but has a slight negative Ce anomaly on an interior sample (Mittlefehldt and Lindstrom, 1991a).
- Clast EET 87503,62 is a heavily fractured, fine-grained basalt clast (Metzler et al, 1995; **Figure 7**). Its pyroxenes are equilibrated, showing augite exsolution lamellae set in pigeonite hosts; compositionally, pyroxenes are Fe- and Ca-rich (average $\sim\text{Wo}_{14}\text{En}_{28}\text{Fs}_{58}$) with high-Na feldspars ($\sim\text{An}_{75-85}$) (Metzler et al, 1995; **Figure 8**). REE patterns are relatively flat compared to CI, with a slight negative Eu anomaly (Metzler et al, 1995; **Figure 9**). Bulk data for this clast is shown in **Table 2**, below.

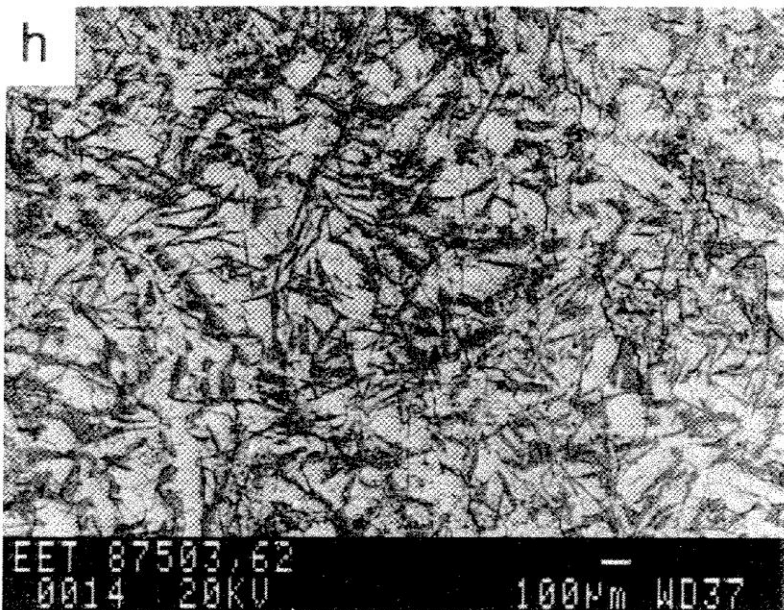


Figure 7: BSE image of fine-grained basalt clast EET 87503,62, with dark plagioclase and lighter pyroxene. Scale bar is 100 μm . From Metzler et al (1995).

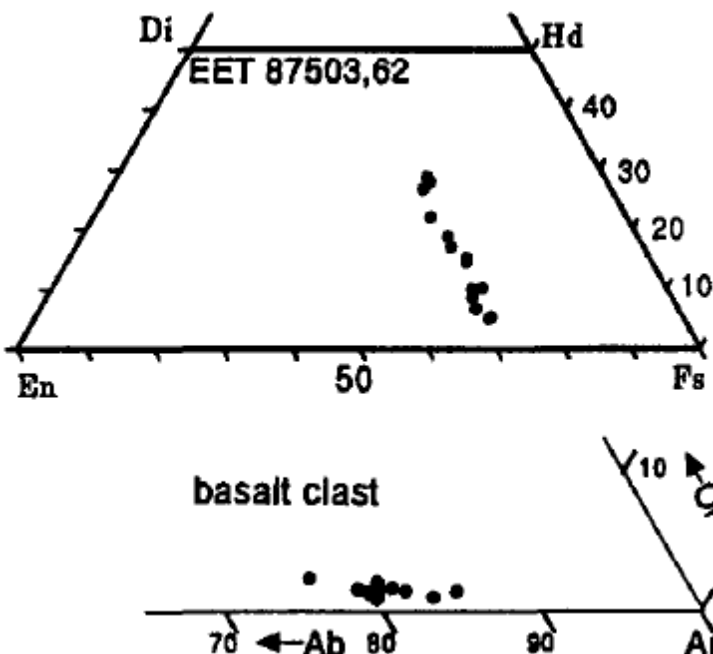


Figure 8: Compositional diagrams for pyroxene (top) and plagioclase (bottom) from fine-grained basalt clast EET 87503,62. From Metzler et al (1995).

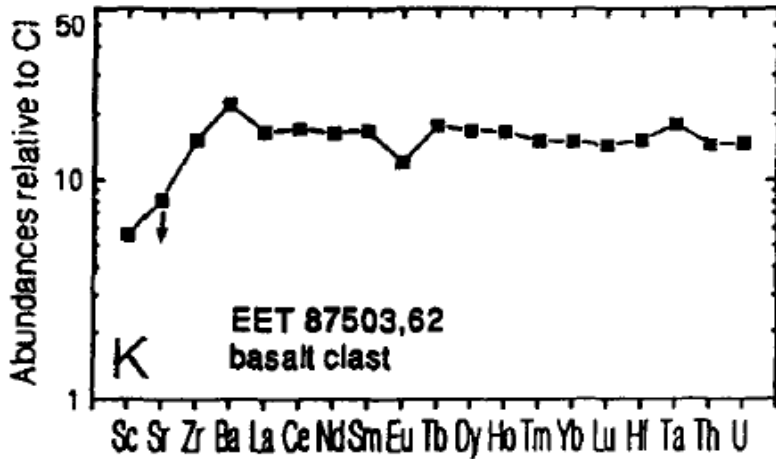


Figure 9: CI-normalized REE abundances from fine-grained basalt clast EET 87503,62, showing mostly flat REE enrichment with a slight negative Eu anomaly. From Metzler et al (1995).

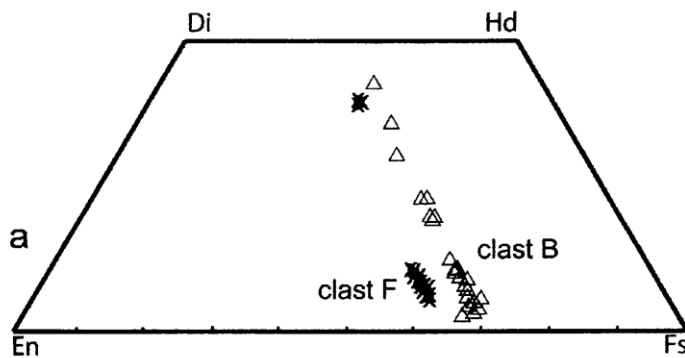
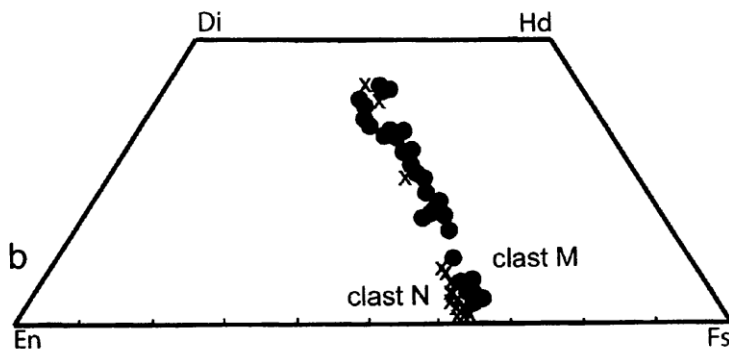


Figure 10: Pyroxene compositions from four different clasts in EET 87503, reported by Buchanan and Mittlefehldt (2003).



- Clast B is impact-modified clast; it has a subophitic to ophitic texture with skeletal feldspars (An_{74-89}) and anhedral, shocked, and blackened Fe-rich pyroxenes ($Mg\# \approx 30$; **Figure 10**) that also display undulose extinction (Buchanan and Mittlefehldt, 2003). A large portion of mesostasis is also present (Buchanan and Mittlefehldt, 2003).

- Clast BA is similar to EET

87513 Clast B (513-B) as a fragment of a Nuevo Laredo trend eucrite (Buchanan and Mittlefehldt, 2003); its bulk composition is shown in **Table 3** and its CI-normalized REE pattern is shown in **Figure 11**.

- Clast F from EET 87503 (**Figure 12**) is a fragment of an equilibrated, main-group eucrite, with pyroxene compositions (**Figure 10**) and CI-normalized REE pattern (**Figure 11**) that are broadly similar to Juvinas (though slightly more Fe-rich) (Buchanan and Mittlefehldt, 2003). Its bulk composition is shown in **Table 3**.
- Clast L is an equilibrated Nuevo Laredo trend eucrite (Buchanan and Mittlefehldt, 2003); its bulk composition is shown in **Table 3**, with REE in **Figure 11**.
- Clast Z from EET 87503 is similar to Clast F as a fragment of a main-group, equilibrated eucrite (Buchanan and Mittlefehldt, 2003); its bulk composition is shown in **Table 3** and its CI-normalized REE pattern is shown in **Figure 11**.

Table 3: Bulk chemistry of five different clasts measured by Buchanan and Mittlefehldt (2003) in EET 87503.

reference	Buchanan and Mittlefehldt 03				
	EET 87503 Clast F	EET 87503 Clast L	EET 87503 Clast M	EET 87503 Clast Z	EET 87503 Clast BA
sample #	,136	,109	,105	,116	,122
total weight	55.2 mg	46.2 mg	40.7 mg	77.1 mg	62.4 mg
Cr ₂ O ₃	0.315	0.283	0.3	0.292	0.369
FeO	19.2	20	19.9	18.4	18.1
MnO	0.57	0.3	0.59	0.37	--
CaO	9.7	10	10	10.3	10.1
Na ₂ O	0.429	0.626	0.501	0.473	0.48
K ₂ O	--	--	--	--	0.042
Sc ppm	30.8	33.7	29.8	30.8	29.4
Co ppm	5.47	6.25	4	3.42	12.2
Ni ppm	--	40	--	--	40
Sr ppm	70	90	90	80	100
La ppm	1.84	4.11	3.35	2.21	3.47
Ce ppm	5.2	10.5	9	6	10.7
Nd ppm	4.0	5.0	6.0	5.0	6.0
Sm ppm	1.27	2.58	2.09	1.5	2.26
Eu ppm	0.54	0.75	0.69	0.65	0.68
Tb ppm	0.32	0.62	0.52	0.4	0.55
Yb ppm	1.62	2.5	2.04	1.84	2.17
Lu ppm	0.246	0.363	0.304	0.27	0.315
Hf ppm	0.93	1.88	1.45	1.24	1.86
Ta ppm	0.082	0.24	0.17	0.21	0.34
Th ppm	0.18	0.43	0.35	0.19	0.47
technique:	INAA	INAA	INAA	INAA	INAA

Impact:

- Clast EET 87503,35 is a black clast; it is howarditic in composition (low Ca and Sc, high Cr), with Co and Ni contents that are similar to the surrounding matrix (Mittlefehldt and Lindstrom, 1991a). Its composition indicates up to 45% diogenitic parent material (Mittlefehldt and Lindstrom, 1991a).
- Clasts EET 87503,63, 87503,68, and 87503,69 are impact melt breccias with mineral fragments up to several hundred μm in size set in a very fine-grained (5 μm) crystallized matrix (Metzler et al, 1995; **Figure 13**). EET 87503,63 has a subophitic texture showing equilibrated groundmass pyroxenes with exsolution lamellae of augite, and a narrow compositional range for the matrix

(Figure 14), whereas EET 87503,68 and 87503,69 have a wider range of mineral compositions, indicating their more polymict nature (Metzler et al, 1995; Figure 15). REE data for the three clasts is flat relative to CI, with a very slight negative Eu anomaly (Metzler et al, 1995; Figure 16). Clasts EET 87503,69 and EET87503,69 show elevated but flat siderophile element

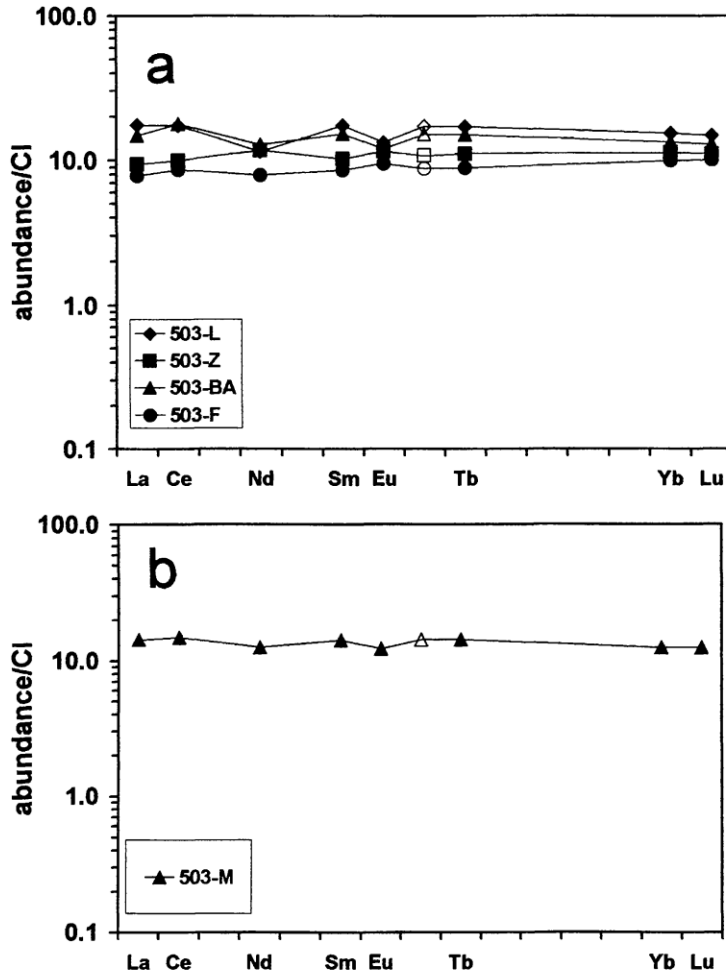


Figure 11: CI-normalized REE abundances for five different clasts from EET 87503, analyzed by Buchanan and Mittlefehldt (2003).

Figure 12: Thin section photomicrograph of Juvinas-like clast F from EET 87503, with a long axis of 1.8 mm. From Buchanan and Mittlefehldt (2003).



concentrations relative to Cl; Au/Ir and Ni/Ir ratios are suggestive of projectile contamination by H or Cl material (Metzler et al, 1995; **Figure 17**). Bulk chemical data for these clasts is shown in **Table 4**, below.

- Clasts C, E, and G are similar to EET 87503,35 (Mittlefehldt and Lindstrom, 1991a). They consist of silicate fragments in a dark, opaque, likely devitrified groundmass; Clast G is compositionally eucritic (Buchanan and Mittlefehldt, 2003).
- Clast M from EET 87503 is a shocked breccia, composed of silicate fragments in a black, glassy matrix; pyroxenes are Fe-rich ($Mg\# \approx 40$; **Figure 10**) and feldspars show evolved compositions (An_{81-93}), and the clast is highly enriched in REE (12-15xCl) with a negative Eu anomaly, consistent with derivation from a Nuevo Laredo-like source (Buchanan and Lindstrom, 2000; Buchanan and Mittlefehldt, 2003). Other clasts similar to this one and EET 87503,35 are noted in Buchanan and Lindstrom (2000). The bulk composition of clast M is shown in **Table 3**, with the Cl-normalized REE pattern in **Figure 11**.
- Clast N from EET 87503 is broadly similar to Clast M, with equilibrated, Fe-rich pyroxenes ($Mg\# \approx 39$; **Figure 10**).

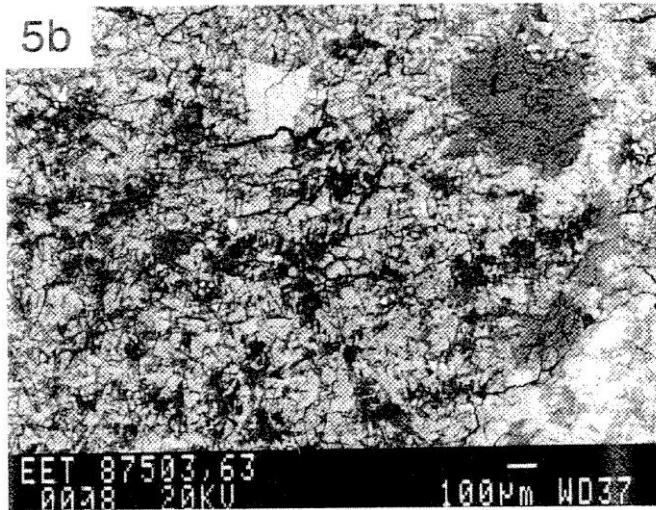
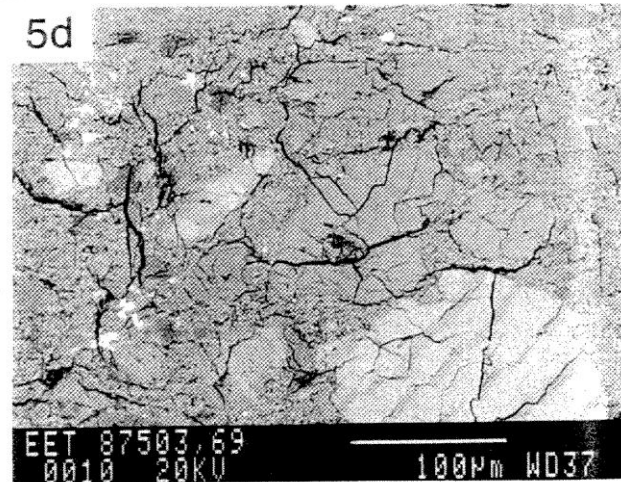
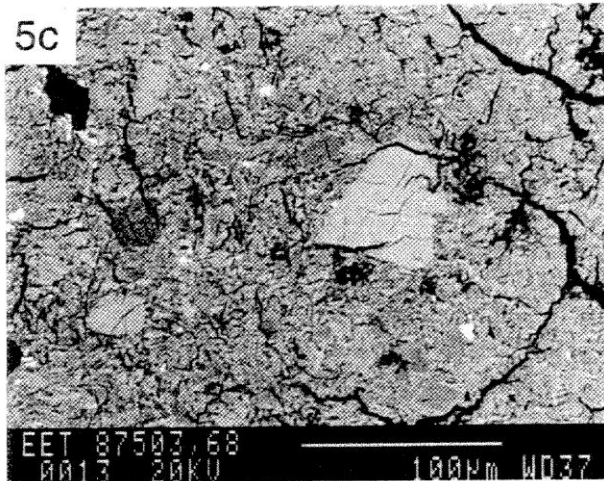


Figure 13: BSE images of three impact melt breccia clasts (EET 87503,63, EET 87503,68, and EET 87503,69), with dark plagioclase and light-gray pyroxene set in a medium-gray, fine-grained matrix. Scale bar at bottom is 100 μm . From Metzler et al (1995).



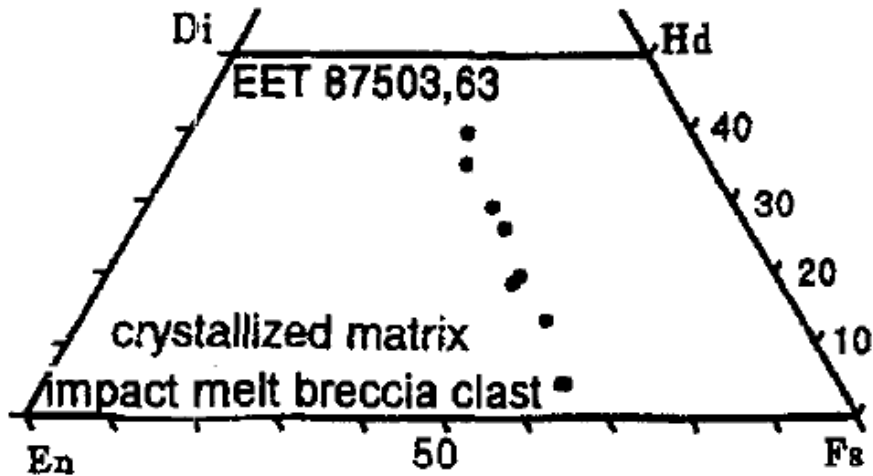


Figure 14: Pyroxene compositions from impact melt breccia clast EET 87503,63, showing a relatively narrow range of pyroxene major-element chemistry. From Metzler et al (1995).

Table 4: Bulk INAA data for clasts EET 87503,63, EET 87503,68, and EET 87503,69, all impact-melt breccias. From Metzler et al (1995).

reference	Metzler et al 95		
	EET 87503,63	EET 87503,68	EET 87503,69
weight	43.6 mg	16.1 mg	39.1 mg
wt% Ca	6.88	4.69	3.9
wt% Fe	15.7	14.6	17
Na ppm	3730	2810	3240
K ppm	312	290	370
Sc ppm	27.9	23.2	19.6
Cr ppm	2246	3850	4290
Mn ppm	4370	3970	3500
Co ppm	5.3	69.5	220
Ni ppm	<15.0	1400	4750
Zn ppm	29.0	28.0	37.0
Ga ppm	1.40	2.10	3.10
Se ppm	<0.40	0.70	2.70
Sr ppm	90.0	<90.0	<60.0
Zr ppm	30.0	<90.0	<40.0
Ba ppm	29.0	<25.0	26.0
La ppm	2.85	1.90	1.56
Ce ppm	7.40	5.00	4.14
Nd ppm	5.50	3.80	3.10
Sm ppm	1.85	1.25	1.00
Eu ppm	0.64	0.40	0.32
Gd ppm	2.60	--	1.30
Tb ppm	0.43	0.29	0.24
Dy ppm	3.00	2.01	1.64
Ho ppm	0.67	0.42	0.37
Tm ppm	0.31	--	0.16
Yb ppm	1.89	1.20	1.01
Lu ppm	0.28	0.17	0.16
Hf ppm	1.19	0.87	0.64
Ta ppm	0.13	0.08	0.04
W ppm	0.15	<0.15	<0.25
Ir ppm	<0.002	0.061	0.205
Au ppm	<0.0003	0.016	0.059
Th ppm	0.340	0.210	0.150
U ppm	0.110	0.070	<0.060
technique	INAA	INAA	INAA

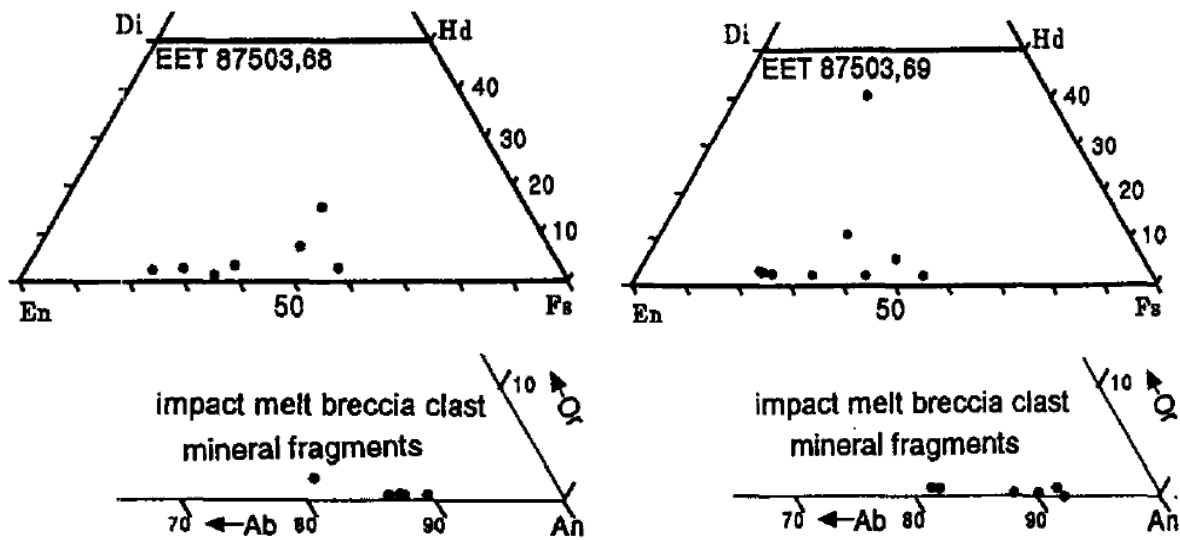


Figure 15: Pyroxene and plagioclase compositions from impact melt breccia clasts EET 87503,68 and EET 87503,69; these clasts show a much wider range of chemistries than EET 87503,63 (Figure 14) and are thus considered polymict breccias. From Metzler et al (1995).

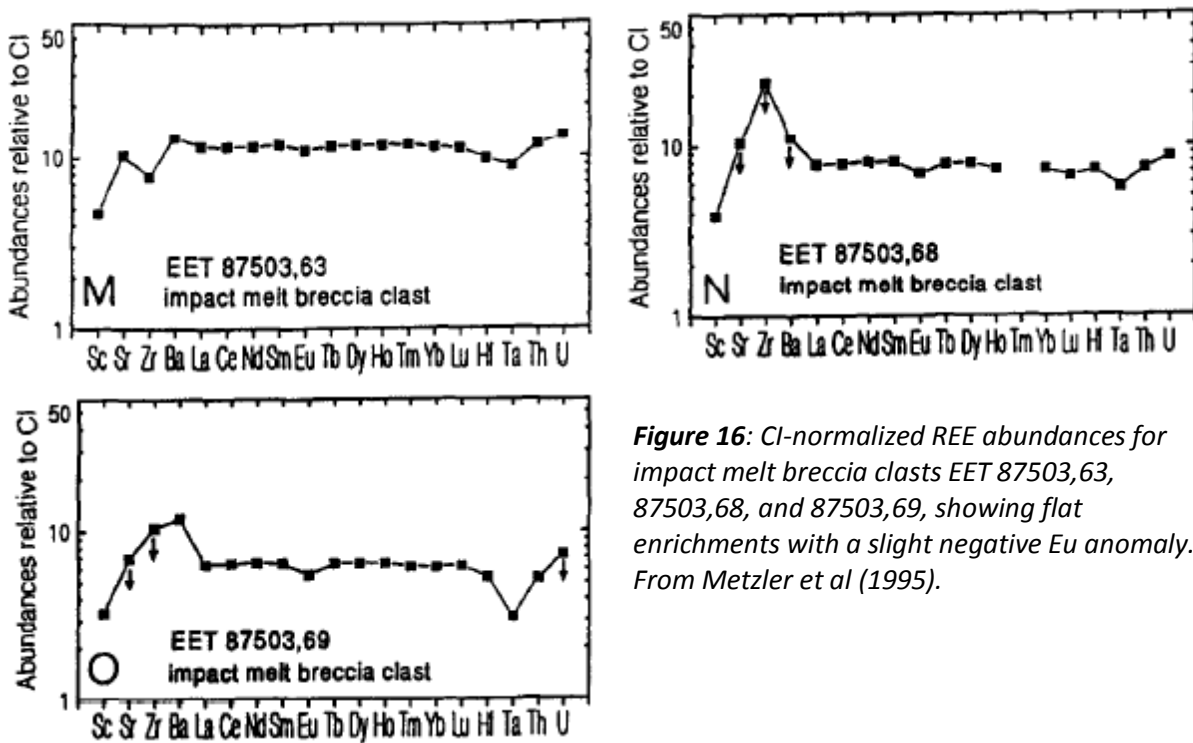
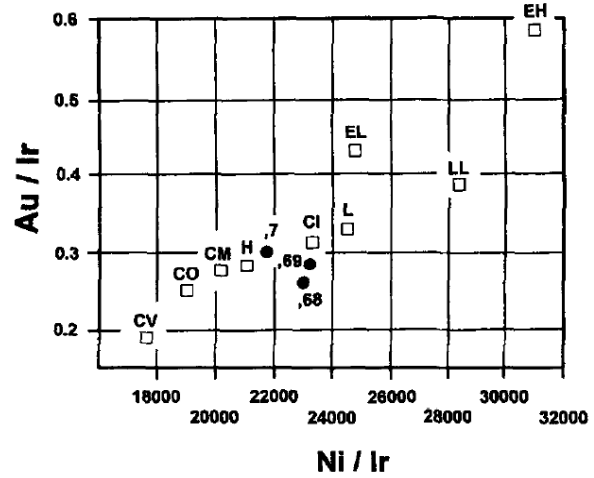
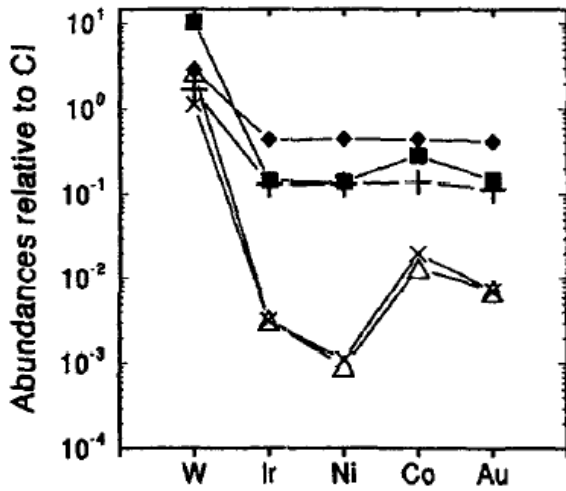


Figure 16: Cl-normalized REE abundances for impact melt breccia clasts EET 87503,63, 87503,68, and 87503,69, showing flat enrichments with a slight negative Eu anomaly. From Metzler et al (1995).



- + EET 87503,68 impact melt breccia clast
- ◆ EET 87503,69 impact melt breccia clast
- Pasamonte 897,7 granulitic breccia clast

- X Stannern basalt clast
- Δ Millbillillie bulk

Figure 17: Two impact melt breccia clasts from EET 87503 (87503,68 and 87503,69) show flat enrichment for siderophile elements (left), suggestive of chondritic contamination; a plot of Au/Ir vs. Ni/Ir ratios (right) indicate that this material is most probably from H or CI chondrites. However, whereas EET 87513 contains clasts of CM2 chondrites, no such clasts have been isolated in EET 87503. From Metzler et al (1995).

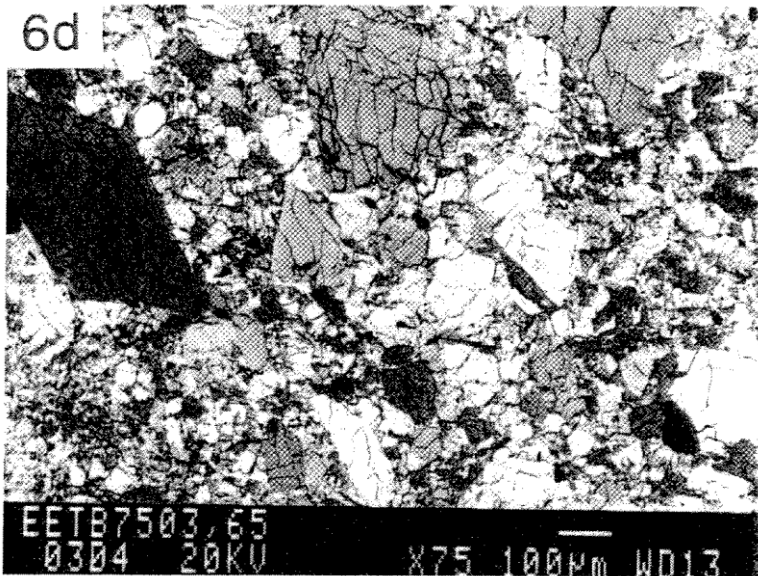


Figure 18: BSE image of the clastic matrix of EET 87503, showing a wide variety of crystal and rock fragments. Note that it is compacted but not recrystallized. From Metzler et al (1995).

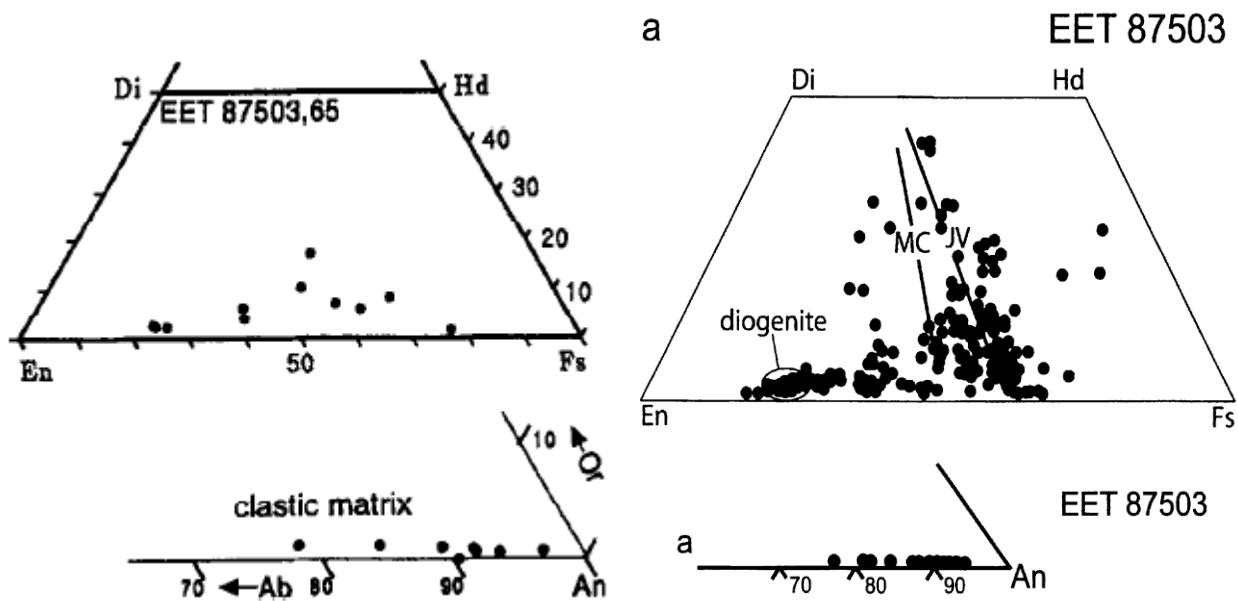


Figure 19: Matrix pyroxene and plagioclase compositions for minerals analyzed in the clastic matrix of EET 87503, showing a wide variety of parent materials from diogenites to highly evolved eucrites. Left set is from Metzler et al (1995), right set is from Buchanan and Mittlefehldt (2003).

EET 87503 Matrix: Pyroxenes in the EET 87503 matrix (**Figure 18**) range from En_{22} (highly fractionated eucrite) to En_{76} (diogenite), with some metastable Fe-rich compositions like those seen in the rims of unequilibrated eucritic pyroxenes (e.g., Pasamonte) and some compositions like those of the cumulate eucrites Binda and Moore County; feldspar compositions range from $\sim An_{78-95}$ (Metzler et al, 1995; Buchanan and Mittlefehldt, 2003; **Figure 19**). Analyses of bulk matrix samples suggest a diogenite component in $\sim 17-20\%$ abundance, with the rest of the meteorite composed of eucritic, impact-altered, or foreign components (Mittlefehldt and Lindstrom, 1991a; Buchanan, 2002; Buchanan and Mittlefehldt, 2003). An inclusion of matrix within a lithic clast (sample ,64) shows compositions that are different from “normal” matrix values, with higher-Ca pyroxenes and a more limited range of An contents (Metzler et al, 1995; **Figure 20**). This unique matrix inclusion was interpreted as a fine-grained breccia sampling a narrower range of HED lithologies than the whole meteorite (Metzler et al, 1995).

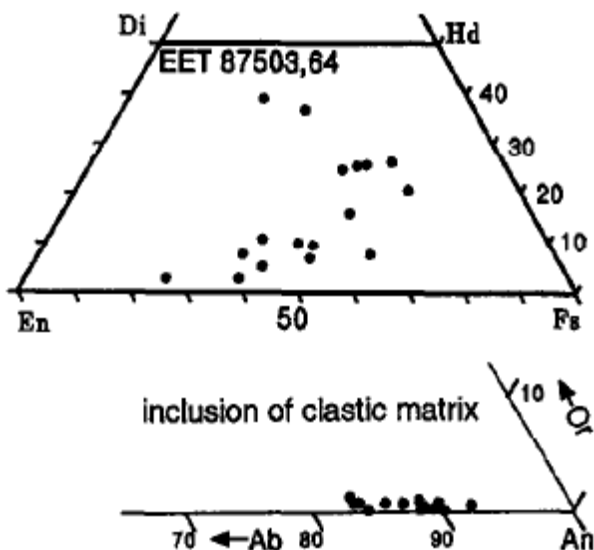


Figure 20: Pyroxene and plagioclase compositions for a sample of “included” matrix (sample 87503,64), showing a slightly different chemistry from the normal matrix (**Figure 19**). From Metzler et al (1995).

EET 87513 Lithics: General information about the variety of pyroxene and plagioclase compositions in EET 87513 is shown in **Figure 21**.

Diogenites:

- Buchanan and Reid (1991) reported an “unnamed” clast from EET 87513 with very Mg-rich pyroxenes ($Mg\# \approx 79$), suggesting a probable diogenitic source.
- Clasts A and EE (more precisely, two fragments of the same clast: Buchanan, 1995) contain fine-grained (<0.45 mm), equigranular, anhedral, twinned, and intergrown orthopyroxenes (En_{70-77} ; **Figure 21**) set in an even finer-grained matrix (~0.1 mm) with equant orthopyroxene, minor olivine (~ Fo_{66}), and very small troilite grains (Buchanan et al, 1990; Buchanan and Reid, 1991; Buchanan, 1995; Buchanan and Mittlefehldt, 2003; **Figure 22**). Some larger pyroxene grains have exsolution lamellae, and there is minor undulatory extinction in both fragments (Buchanan, 1995; Buchanan and Mittlefehldt, 2003). Major and minor chemical data (**Table 5**) is similar to the Ellemeet diogenite, and REE abundances (**Figure 23**) are 1-2xCI with a positive Ce anomaly (Buchanan, 1995; Buchanan and Mittlefehldt, 2003). They were interpreted as brecciated, recrystallized, weathered, and metamorphosed diogenitic orthopyroxenites (Buchanan et al, 1990; Buchanan, 1995; Buchanan and Lindstrom, 2000; Buchanan et al, 2002; Buchanan and Mittlefehldt, 2003). Clast 9 is also very similar to A and EE (Buchanan and Lindstrom, 2000; Buchanan and Mittlefehldt, 2003; **Figure 21**).

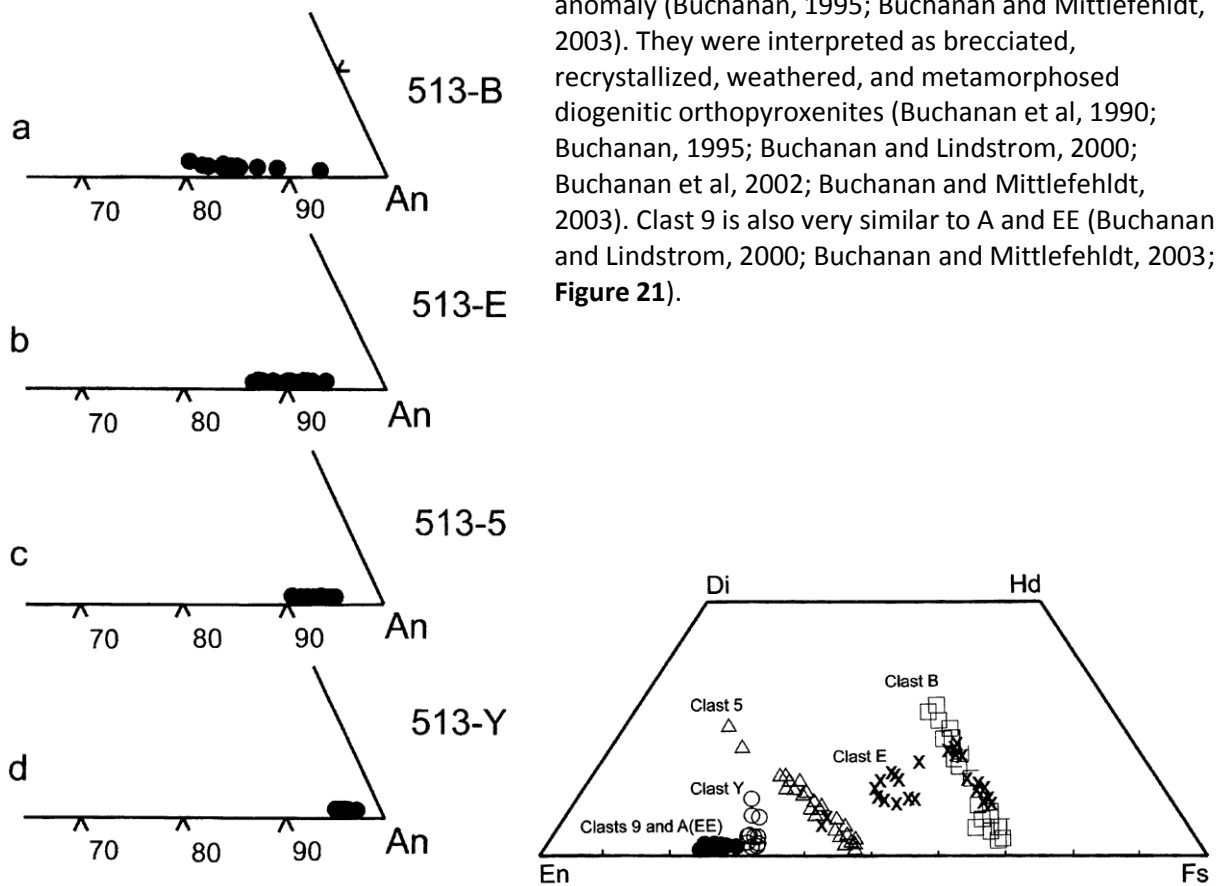
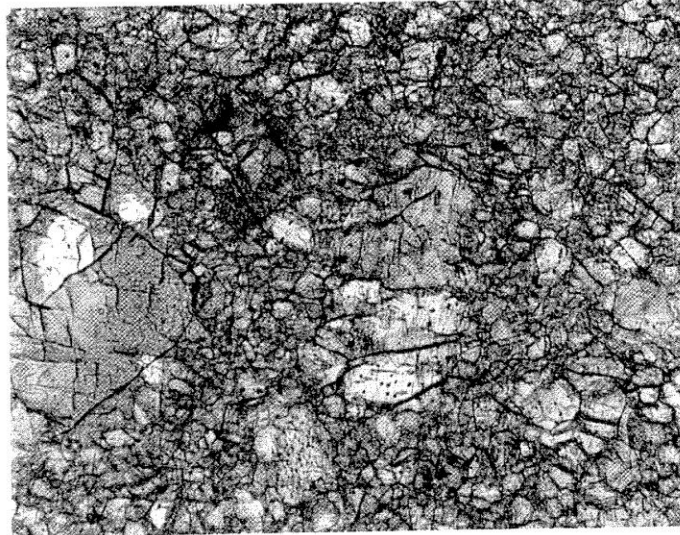


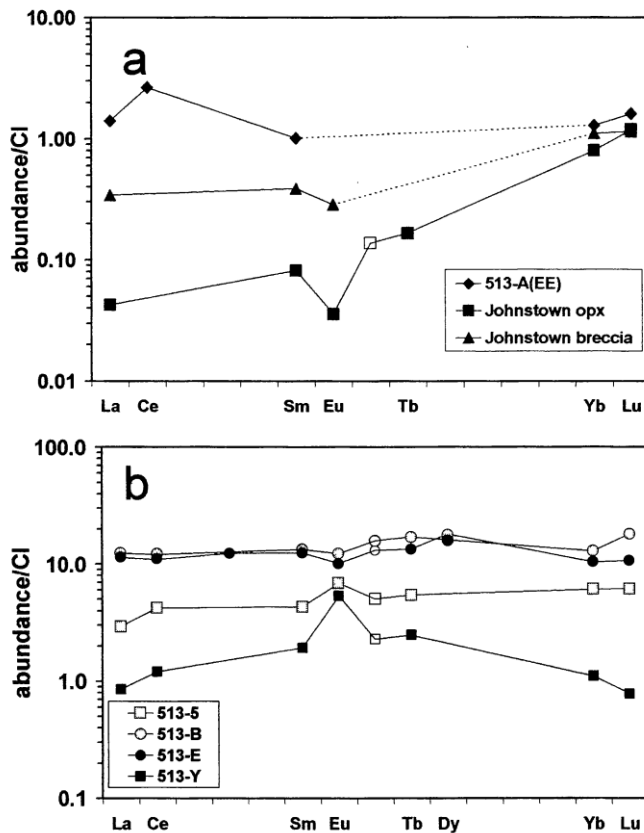
Figure 21: Pyroxene and plagioclase compositions from different clasts in EET 87513, showing the wide variety of clasts present in the meteorite (no plagioclase was found in diogenite clasts 9, A, or EE). From Buchanan and Mittlefehldt (2003).

Figure 22: Thin section photomicrograph of diogenite breccia clasts A/EE (clast 9 is also very similar). Long axis of the photo is 1 mm. From Buchanan and Mittlefehldt (2003).



Eucrites:

- Clast B is a fine-grained (0.2-1.0 mm), subophitic, equilibrated and deformed eucrite clast (Buchanan et al, 1990; Buchanan, 1995). Pyroxenes in this clast are irregular and Fe-rich (Mg# ≈ 30-41; see **Figure 21**) similarly to Nuevo Laredo, and have thin, non-uniform, curved, and discontinuous exsolution lamellae;



exsolution is more common in pyroxene cores, which may be related to relict Ca-zoning (Buchanan et al, 1990; Buchanan, 1995). Blocky feldspars (An₈₂₋₈₉; **Figure 21**) are clouded with inclusions, and ilmenite is also present, with no mesostasis (Buchanan et al, 1990; Buchanan and Reid, 1991). High strain is indicated by undulatory extinction and mosaic texture (Buchanan, 1995). Bulk chemistry (**Table 5**) and chondrite-normalized REE abundances (~10xCl with a negative Eu anomaly; **Figure 23**) are similar to Nuevo Laredo, though Clast B is distinctly more Fe-rich and LREE-poor than Nuevo Laredo (Buchanan, 1995; Buchanan and Lindstrom, 2000; Buchanan and Mittlefehldt, 2003). Thus, this clast is a highly evolved but metamorphosed eucrite (Buchanan, 1995).

Figure 23: Cl-normalized REE abundances in clasts from EET 87513, with the diogenite clast(s) shown above (compared to Johnstown) and the eucrite clasts below. From Buchanan and Mittlefehldt (2003).

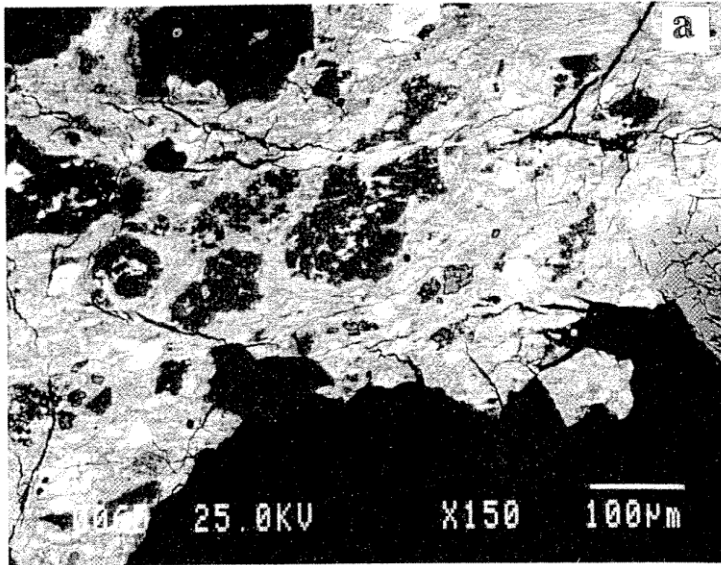


Figure 24: BSE image of clast N, a CM2 chondrite, from EET 87513. Matrix sulfides and phyllosilicates (light) form a flowing texture that wraps around silicate grains, chondrules, and aggregates (dark). From Buchanan et al (1993b).

- Clast E is a fine-grained (0.2-1.0 mm), heavily fractured, unequilibrated eucrite that contains pyroxene ($Wo_7En_{54} - Wo_{22}En_{28}$; **Figure 21**), plagioclase ($\sim An_{87-94}$; **Figure 21**), cristobalite, ilmenite, and chromite (Buchanan and Reid, 1991; Buchanan, 1995). Pyroxenes are equant to elongated, plagioclase is lath-shaped to blocky, and both preserve compositional zoning, though the associated optical effects in pyroxene grains are obscured by strained extinction due to intense fracturing (Buchanan, 1995). Mg-rich pyroxene (cores) show no evidence of exsolution but Fe-rich pyroxene (rims) have fine exsolution lamellae, indicative of partial re-equilibration after initial crystallization (Buchanan, 1995). Bulk chemistry (**Table 5**) and chondrite-normalized REE patterns (10-13xCI with a small negative Eu anomaly; **Figure 23**) are similar to Juvinas (Buchanan, 1995; Buchanan and Mittlefehldt, 2003). This clast is one of the few that has been dated (see below), revealing an early crystallization age (Sm-Nd: 4.53 ± 0.02 Ga; Nyquist et al, 1992) with later Ar degassing (3.4-3.9 Ga; Bogard and Garrison, 1992). Buchanan (1995) interpreted this clast as a main-group eucrite that has been annealed and deformed.
- Clast Y is a recrystallized and deformed eucrite clast with Mg-rich, Ca-poor pyroxene ($Wo_{2-12}En_{63-68}$; **Figure 21**) and high-Ca plagioclase (An_{96-97} ; **Figure 21**), approaching compositions seen in diogenites (Buchanan et al, 1990; Buchanan and Reid, 1991; Buchanan, 1995; Buchanan and Mittlefehldt, 2003). Feldspar and pyroxene grains are aggregates of subgrains with slightly different orientations (i.e., a mosaic texture); grain boundaries are indistinct in feldspars, except for relict twinning, indicating an original fine-grained texture (0.2-1.0 mm grain size) (Buchanan, 1995). Some mineral grains show extreme undulatory extinction, suggestive of high strain (Buchanan, 1995). Bulk chemical data (**Table 5**) shows less Ca and Al but similar REE patterns (**Figure 23**) to the Serra de Mage cumulate eucrite (0.9-2xCI with a positive, 5xCI Eu anomaly) (Buchanan, 1995; Buchanan and Lindstrom, 2000; Buchanan and Mittlefehldt, 2003). This clast has been interpreted as an Mg-rich, shock-deformed eucrite that is related to, but distinct from, the cumulate eucrites (most notable in its lack of cumulate texture) (Buchanan, 1995; Buchanan et al, 2002).
- Clast 5 is similar to Clast Y with high-Mg pyroxene and Ca-rich feldspar (**Figure 21**); it was originally a medium-grained rock but experienced an episode of metamorphism that

recrystallized its pyroxene and feldspar to a finer grain size (Buchanan and Mittlefehldt, 2003). Its composition is shown in **Table 5**, with its REE pattern (3-6xCl with 6.9xCl Eu enrichment, similar to Moore County: Buchanan and Mittlefehldt, 2003) in **Figure 23**. This clast is probably derived from a cumulate eucrite parent rock (Buchanan and Mittlefehldt, 2003).

- Clast X is a large fragment (3x2 mm) of a Binda-like, low-Ca, Mg-rich pyroxene with blebby augite exsolution lamellae (Buchanan and Mittlefehldt, 2003).

Table 5: Bulk INAA data for clasts A/EE, B, E, Y, and 5 from EET 87513.
From Buchanan (1995) and Buchanan and Mittlefehldt (2003).

reference clast sample	Buchanan 95; Buchanan and Mittlefehldt 03				
	EET 87513, Clast A/EE	EET 87513, Clast B	EET 87513, Clast E	EET 87513, Clast Y	EET 87513, Clast 5
total weight	38.7 mg	42.8 mg	34.7 mg	59.2 mg	50.3 mg
TiO ₂	--	0.54	--	--	--
Al ₂ O ₃	--	11.9	13.5	16	--
FeO	17.6	23.6	18.5	10.4	17.4
MnO	0.57	0.63	0.59	0.37	--
CaO	0.91	10.4	11.3	10.6	8.8
Na ₂ O	0.0152	0.54	0.37	0.197	0.259
K ₂ O	--	0.065	0.036	0.0094	--
Cr ₂ O ₃	0.902	0.313	0.447	0.358	0.393
Sc ppm	12.5	36.4	39.8	13.9	23.0
V ppm	134	78	--	99	--
Co ppm	21.4	4.7	9.8	9.6	12.1
Ni ppm	55	42	28	21	37
Sr ppm	--	106	91	73	59
La ppm	0.33	2.91	2.67	0.20	0.689
Ce ppm	1.6	7.3	6.6	0.73	2.54
Nd ppm	--	--	5.6	--	--
Sm ppm	0.149	1.97	1.84	0.284	0.637
Eu ppm	--	0.69	0.57	0.3	0.385
Tb ppm	--	0.62	0.49	0.09	0.20
Dy ppm	--	3.9	4.4	--	--
Yb ppm	0.21	2.1	1.70	0.18	0.99
Lu ppm	0.039	0.44	0.26	0.019	0.149
Hf ppm	--	1.5	1.16	--	0.55
Ta ppm	--	0.21	0.15	--	0.04
Th ppm	--	0.38	0.51	--	--
Au ppb	--	2.2	4.4	2.3	--
technique:	INAA	INAA	INAA	INAA	INAA

Impact:

- Buchanan and Mittlefehldt (2000) mention several clasts that are composed of silicate fragments in a black and glassy matrix, but the authors not describe these in depth; they are similar to the impact breccias from Metzler et al (1995) and clast EET 87503,35 from Mittlefehldt and Lindstrom (1991a).
- Clast 6 is a polymict breccia with a wide range of pyroxene compositions (Buchanan and Mittlefehldt, 2003).
- Clast BC is a polymict breccia similar to Clast 6 (Buchanan and Mittlefehldt, 2003).
- Clast 8 is an extensively shocked, brecciated, and metamorphosed clast with Mg-rich, blackened pyroxenes (Buchanan and Mittlefehldt, 2003).

Other:

- Clast N (**Figure 24**) is a 4x5 mm carbonaceous chondrite clast resembling those found in Bholgati (Buchanan et al, 1990), with up to 250 μm diameter silicates in chondrules and aggregates set in a finer-grained matrix (~75 vol% of the clast) with abundant opaques and sulfides (Zolensky et al, 1992; Buchanan et al, 1993a, 1993b; Buchanan, 1995). The matrix forms a flowing, undulating texture that wraps around silicate grains, chondrules, and aggregates (Buchanan et al, 1993a, 1993b; Buchanan, 1995), and some aggregates contain small amounts of glassy or microcrystalline brown mesostasis (Buchanan et al, 1993b; Buchanan, 1995). Silicates include Fe-poor olivine (Fo_{60-89}) and orthopyroxene ($\text{En}_{90-98}\text{Wo}_{1-5}$) (Buchanan et al, 1990; Zolensky et al, 1992; Buchanan et al, 1993a, 1993b; Buchanan, 1995), and the predominant matrix mineral is “flaky and platy” serpentine ($\text{Mg}/\text{Fe} \approx 1.15$) with a maximum grain size of 350 nm (Zolensky et al, 1992; Buchanan et al, 1993a, 1993b; Buchanan, 1995). The serpentine shows 7Å basal lattice fringes that are corrugated with abundant edge dislocations, suggestive of 300-400°C heating (Zolensky et al, 1992; Buchanan et al, 1993a, 1993b; Buchanan, 1995; **Figure 25**); intergrown saponite is present, indicative of high water:rock ratios or high temperature during aqueous alteration (Zolensky et al, 1992; Buchanan et al, 1993a, 1993b; Buchanan, 1995). Accessory matrix minerals include pyrrhotite, pentlandite, enstatite (~ En_{97}), olivine (Fo_{90-100}), diopside, chromite, tochilinite, and tochilinite-serpentine; two other interesting features are irregular to rounded, CaCO_3 -rich, 8-18 μm carbonate grains, and poorly-crystalline, ~100- μm sized carbonaceous spheres (Zolensky et al, 1992; Buchanan et al, 1993a, 1993b; Buchanan, 1995). The bulk composition of clast N, though anomalously Sm- and Au-enriched and Lu-depleted, suggests a CM2 chondrite (Buchanan et al, 1993a, 1993b; Buchanan, 1995; **Figure 26**), which is supported by oxygen isotope analyses (see below). Chemical analyses of carbonate grains, the opaque-rich matrix, and a bulk sample are shown below in **Table 6**.
- Clast 7 is another CM2 fragment, first reported by Buchanan and Lindstrom (2000). Most elements are 1-2xCI, though Na is depleted (0.34xCI) (Buchanan and Lindstrom, 2000; Buchanan and Mittlefehldt, 2003; **Table 6**).
- Recently, one group of researchers (Fukawa et al, 2005) reported finding 26 distinct carbonaceous chondrite clasts in EET 87513, ranging in size from 18 μm x 22 μm to 500 μm x 700 μm , with an average of 90 x 132 μm . Twenty-five of these clasts were determined to be CM material, but one was noted as a CI chondrite, with framboidal aggregates of magnetite in a fine-grained matrix (Fukawa et al, 2005). The CM clasts were analyzed with X-ray diffraction and are composed of serpentine, olivine, low-Ca pyroxene, “calcite” (perhaps referring to the carbonate grains reported in clast N), and kamacite (Fukawa et al, 2005); excluding kamacite, these clasts are very similar to clast N and clast 7.



Figure 25: TEM image of matrix serpentine flakes in EET 87513, clast N. 7Å basal lattice fringes are shown, with corrugation in one flake marked by the black arrow. From Buchanan et al (1993b).

Table 6: Analyses of carbonate grains, the opaque-rich matrix, and a bulk sample from EET 87513, Clast N, a CM2 chondrite; also included is an analysis of Clast 7, another CM2 fragment. From Buchanan et al (1993b), reprinted in Buchanan (1995); Clast 7 from Buchanan and Mittlefehldt (2003).

reference	Buchanan et al 93b, Buchanan 95 EET 87513, CLAST N			Buchanan and Mittlefehldt 03 EET 87513, Clast 7 (Sample ,118)		
comments	carbonate grain	carbonate grain	carbonate grain	matrix	bulk	bulk
SiO ₂	--	--	--	24.6	--	--
TiO ₂	--	--	--	0.08	--	--
Al ₂ O ₃	--	--	--	2.74	2.67	--
FeO	0.99	0.45	0.80	36.5	30.0	27.9
MnO	0.1	0.67	0.00	0.20	0.23	--
MgO	0.03	0.00	0.03	13.9	22	--
CaO	55.0	55.6	55.3	0.72	2.3	1.5
Na ₂ O	--	--	--	0.26	0.260	0.228
K ₂ O	--	--	--	0.03	0.034	--
Cr ₂ O ₃	--	--	--	0.30	0.506	0.469
SO ₃	--	--	--	11.1	--	--
P ₂ O ₅	--	--	--	0.14	--	--
NiO	--	--	--	1.66	1.72	1.58
CO ₂ (stoic.)	43.9	44.4	43.9	--	--	--
Sum (reported)	100.0	101.1	100.0	92.2	--	--
Sc ppm	--	--	--	--	9.3	7.98
V ppm	--	--	--	--	78	--
Co ppm	--	--	--	--	628	590
La ppm	--	--	--	--	0.41	0.597
Ce ppm	--	--	--	--	1.4	1.7
Sm ppm	--	--	--	--	0.46	0.322
Eu ppm	--	--	--	--	--	0.089
Tb ppm	--	--	--	--	--	0.08
Yb ppm	--	--	--	--	0.25	0.32
Lu ppm	--	--	--	--	0.024	0.052
Ir ppb	--	--	--	--	570	--
Au ppb	--	--	--	--	255	246
technique:			EPMA			INAA

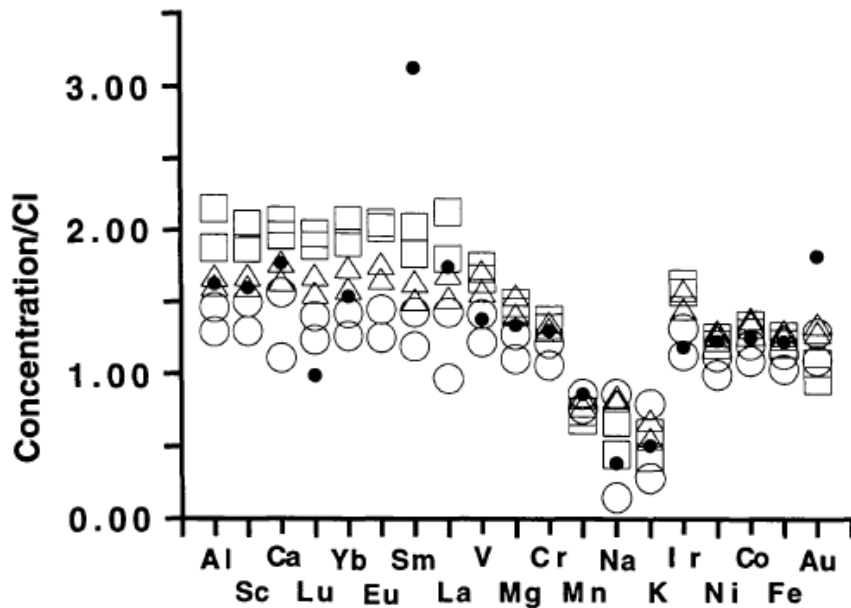


Figure 26: Lithophile and siderophile element abundances from EET 87513, clast N, which is marked by solid dots. Other sets of symbols mark minima and maxima for CM (circles), CO (triangles), and CV (squares) carbonaceous chondrites. Though there are some outliers (e.g., Sm, Au, and Lu), the clast data is consistent with CM chondrites. From Buchanan et al (1993b).

EET 87513 Matrix: Pyroxene chemistry in the EET 87513 matrix (**Figure 27**) shows a bimodal Mg# distribution, ranging from ~34-85, suggestive of significant contributions from both diogenitic and eucritic components with a wide range of chemistries, including contributions from unequilibrated eucrites (Fe-rich) and cumulate eucrites, similarly to EET 87503 (Buchanan, 1995; Buchanan and Mittlefehldt, 2003; **Figure 28**). The bulk composition of the EET 87513 matrix is shown in **Table 7**. EET 87513 is more Cr-rich and Ca- and Sc-poor than the polymict eucrites (e.g., EET 87509 and EET 87531), indicating a greater diogenitic component of 22-35% compared to <10% for polymict eucrites (Mittlefehldt and Lindstrom, 1991a; Buchanan, 2002; Buchanan and Mittlefehldt, 2003). The Al_2O_3 content of EET 87513 is similar to howardites but lower than polymict eucrites, and REE distributions are similar to Bholgati and Kapoeta, further supporting the interpretation that EET 87513 is a howardite (Buchanan, 1995).

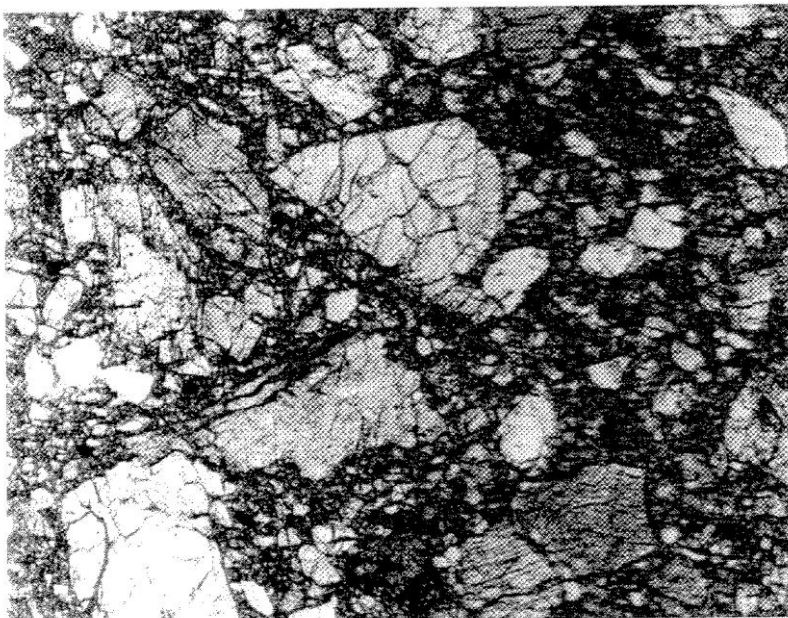


Figure 27: Plane-polarized light photomicrograph of the EET 87513 matrix. The long axis of the photo is 1.8 mm. From Buchanan and Mittlefehldt (2003).

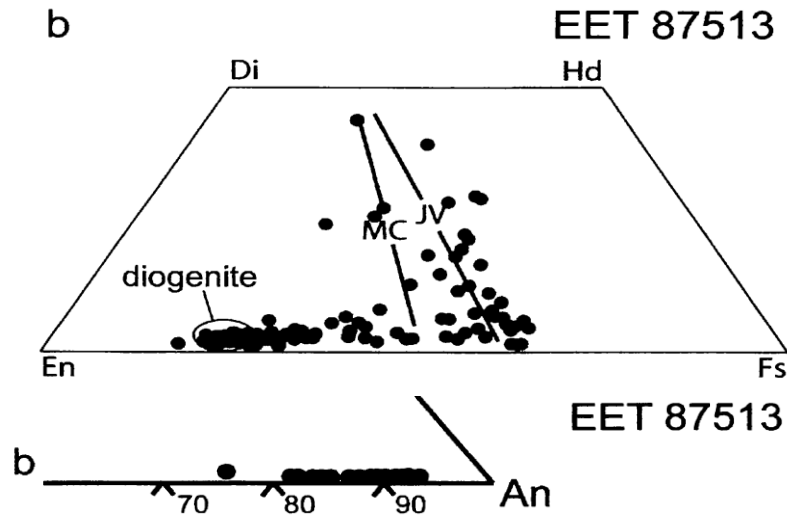


Figure 28: Pyroxene and plagioclase compositions from the matrix of EET 87513, showing a wide variety of parent materials (from diogenites to highly evolved eucrites) similarly to EET 87503. From Buchanan and Mittlefehldt (2003).

Table 7: Bulk INAA analysis of the EET 87513 matrix. From Buchanan (1995), reprinted in Buchanan and Mittlefehldt (2003).

reference	Buchanan 95
	EET 87513, MATRIX
comments	wtd. avg. of 3 samples
total weight	194.8 mg
TiO ₂	0.43
Al ₂ O ₃	8.4
FeO	19.1
MnO	0.53
CaO	7
Na ₂ O	0.30
K ₂ O	0.026
Cr ₂ O ₃	0.763
Sc ppm	24.7
V ppm	101
Co ppm	27.8
Ni ppm	273
Sr ppm	57
La ppm	1.91
Ce ppm	5.1
Nd ppm	4.8
Sm ppm	1.29
Eu ppm	0.39
Tb ppm	0.34
Dy ppm	1.8
Yb ppm	1.14
Lu ppm	0.19
Hf ppb	880
Ta ppb	120
Ir ppb	9
Au ppb	4.2
Th ppb	240
technique:	INAA

Whole-Rock Chemistry: Though more comprehensive and perhaps more informative chemical analyses have been focused on individual clasts and the matrix of EET 87503 and EET 87513, at least one worker has reported whole-rock chemical data for major elements in EET 87503 (Jarosewich, 1990). Whole-rock Cl abundances were reported for both meteorites by Garrison et al (2000), with data for high-T, low-T, and total Cl; however, the values for total chlorine (EET 87503 = 6-15 ppm Cl, EET 87513 = 13-15 Cl) are in most cases less than or equal to the error for the measurements (EET 87503 = 19-22 ppm uncertainty, EET 87513 = 10-15 ppm uncertainty).

Radiogenic Isotopes: Bogard and Garrison (1992) investigated ^{39}Ar - ^{40}Ar systematics in two samples from EET87513 (sample ,82 = clast P and sample ,18 = clast E); while one sample (clast P) gave a reasonably well-defined plateau age of ~ 3.7 Ga (**Figure 29**), both samples showed a significant range of apparent ages with increasing temperature of Ar release, from ~ 3.4 - 3.5 at low T to ~ 4.1 at high T (Bogard and Garrison, 1992; Bogard, 1995). A similar Ar-Ar plateau age was determined for sample ,53 from EET 87503 (~ 3.7 Ga), while another sample (,23) was used to construct an isochron of 4.41 ± 0.02 Ga (Bogard, 1995). The range of ages presented here can be taken as possible ages for major degassing or impact events on the HED parent body (Bogard and Garrison, 1992; Bogard, 1995).

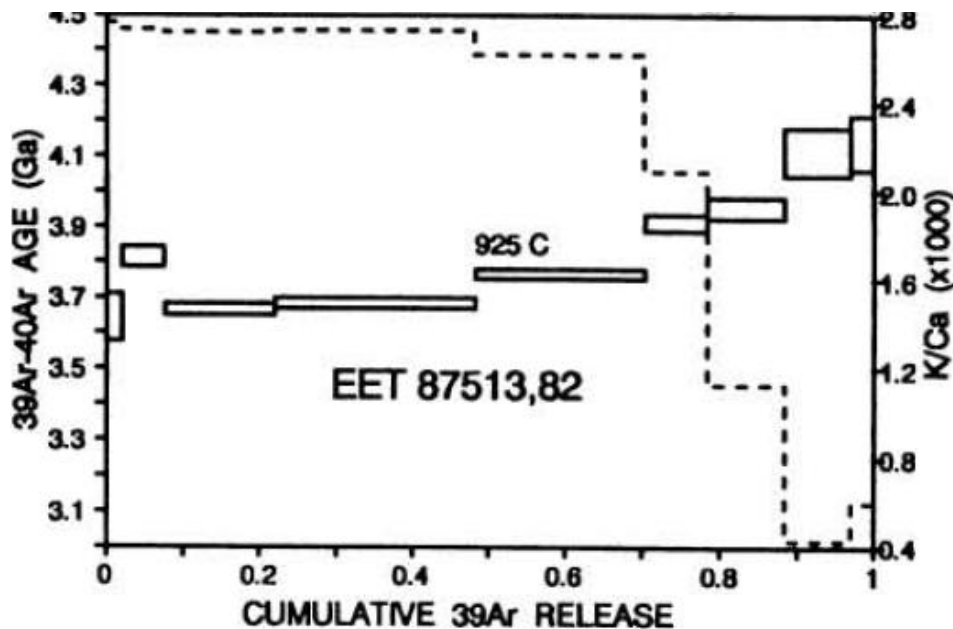


Figure 29: Cumulative Ar release diagram for EET 87513,82 (clast P); this spectrum defines a plateau age of ~ 3.7 Ga, which is inferred as the timing of major Ar degassing for the sample. From Bogard and Garrison (1992).

Nyquist et al (1992) reported a Sm-Nd crystallization age of 4.53 ± 0.02 Ga from EET 87513,18, clast E (**Figure 30**); this clast was chosen for lack of textural evidence for terrestrial weathering, and clasts that plot off the isochron (Q, J, and R) are displaced according to the amount of trivalent LREE depletion during weathering (Nyquist et al, 1992). Nyquist et al (1994) followed up with a concordant Rb-Sr age for clast E from EET 87513,18 of 4.49 ± 0.08 Ga (**Figure 31**). These ages indicate that though EET 87513,18, clast E experienced significantly Ar resetting (see above), other isotopic systems were not majorly affected.

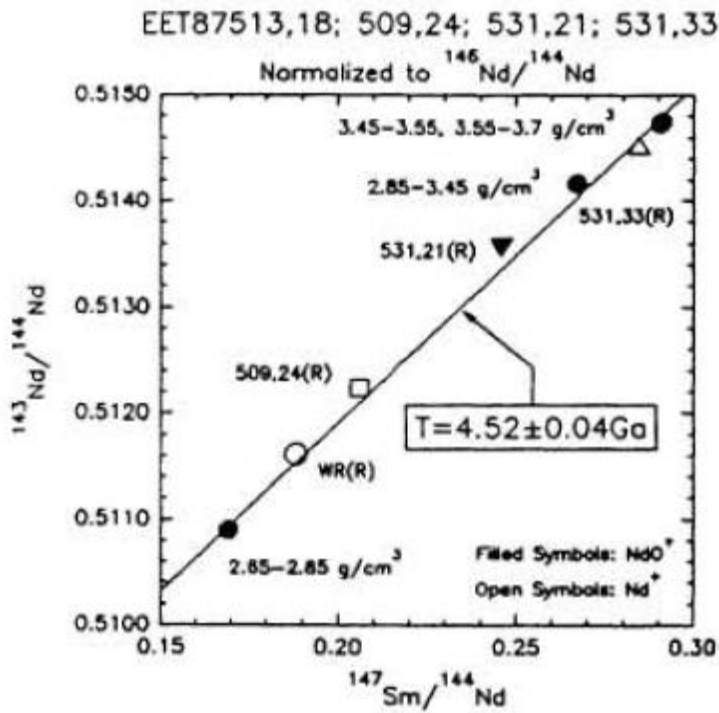


Figure 30: Sm-Nd isochron diagram for EET 87513,18 (clast E), with some data for EET 87509 and EET 87531, which have since been ruled out as pairs of EET 87513 (Buchanan et al, 2000). The best-fit line describes an isochron at 4.52 ± 0.04 Ga (or 4.53 ± 0.04 Ga depending on the points used). From Nyquist et al (1992).

The same study (Nyquist et al, 1994) reported preliminary Rb-Sr and Sm-Nd ages for EET 87503, sample ,53. This sample also experience Ar resetting

(see above), but unlike clast E from EET 87513, its Rb-Sr and Sm-Nd systems were also affected, resulting in apparent ages of ~ 2.3 - 3.5 Ga (Rb-Sr) or 2.9 ± 1.1 Ga (Sm-Nd) (Nyquist et al, 1994). However, an examination of ^{146}Sm - ^{142}Nd systematics (as opposed to the conventional ^{147}Sm - ^{143}Nd system used for dating) revealed a similar $^{146}\text{Sm}/^{144}\text{Sm}$ ratio to clast E from EET87513 (EET87503,53: 0.0061 ± 0.0007 , EET87513,18: 0.066 ± 0.0009), indicating that the crystallization ages are actually very close (Nyquist et al, 1994). One possible reason for the differences in isotopic disturbances between such similarly-aged clasts may be related to pyroxene equilibration, as clast E from EET87513 is much less equilibrated than sample ,53 from EET87503 (Nyquist et al, 1994).

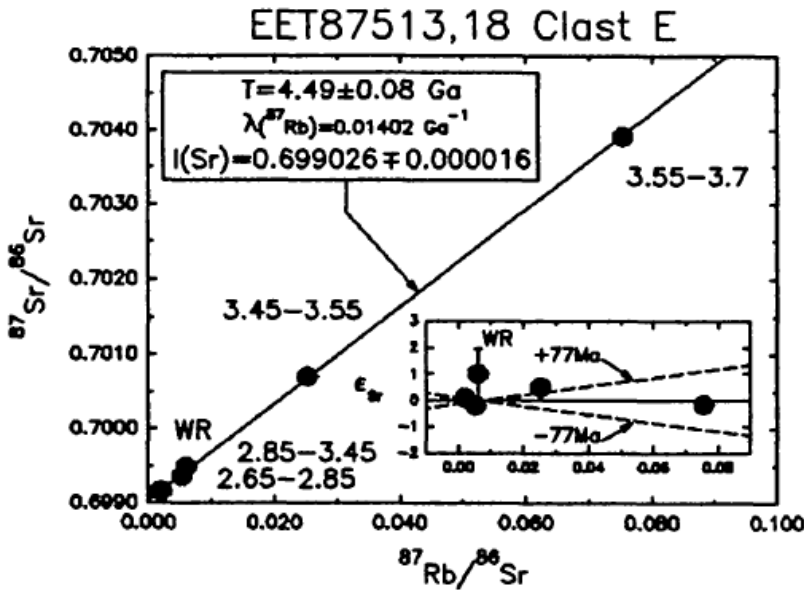


Figure 31: Rb-Sr isochron diagram for EET 87513,18 (clast E), with a best-fit age of 4.49 ± 0.08 Ga. From Nyquist et al (1994).

Cosmogenic Isotopes: Metzler et al (1995) mentions that EET 87503 has a large trapped solar gas component from its residence time in the parent body regolith, suggesting that the meteorite was not heated significantly after aggregation, but no quantitative data on cosmogenic isotopes or cosmic-ray exposure ages are available in the literature for either EET87503 or EET87513.

Other Isotopes: The oxygen isotope composition of EET87513 Clast N (the 4 mm x 5 mm carbonaceous chondrite fragment) was reported by Buchanan et al (1993a, 1993b), with $\delta^{18}\text{O}_{\text{SMOW}} = 5.14\text{‰}$ and $\delta^{17}\text{O}_{\text{SMOW}} = -0.46\text{‰}$. These values plot within the isotopic range defined by CM chondrites (Buchanan et al, 1993a, 1993b; **Figure 32**). A bulk oxygen isotope analysis of EET87513 revealed values ($\delta^{18}\text{O} = 3.11\text{‰}$, $\delta^{17}\text{O} = 1.45\text{‰}$, $\Delta^{17}\text{O} = -0.17\text{‰}$) that were similar to other HED meteorites ($\Delta^{17}\text{O}_{\text{HOWARDITE}} = -0.26\text{‰} \pm 0.08\text{‰}$, $\Delta^{17}\text{O}_{\text{HED}} = -0.25\text{‰} \pm 0.08\text{‰}$) (Clayton and Mayeda, 1996).

Experiments: Natural thermoluminescence was investigated in one sample of EET 87503 (sample ,3) and five samples of EET 87513 (samples 2, 78, 91, 96, and 100) by Sears et al (1991). They found similar TL responses for the two meteorites at 250°C (EET 87503,3 = 6.1 ± 0.8 krad and EET 87513 mean = 7 ± 1 krad), but rather different sensitivities at 400°C (EET 87503,3 = 24 ± 5 krad and EET 87513 mean = 13 ± 6 krad), though two 400°C TL values for EET 87513 were concordant with EET 87503,3 (EET 87513,2 = 18 ± 5 krad @ 400°C, EET 87513,78 = 22 ± 1 krad @ 400°C). EET 87528, another possible pair of the group, produced TL values similar to both meteorites (EET 87528,5 = 5.1 ± 0.8 krad @ 250°C, 21 ± 4 krad @ 400°C).

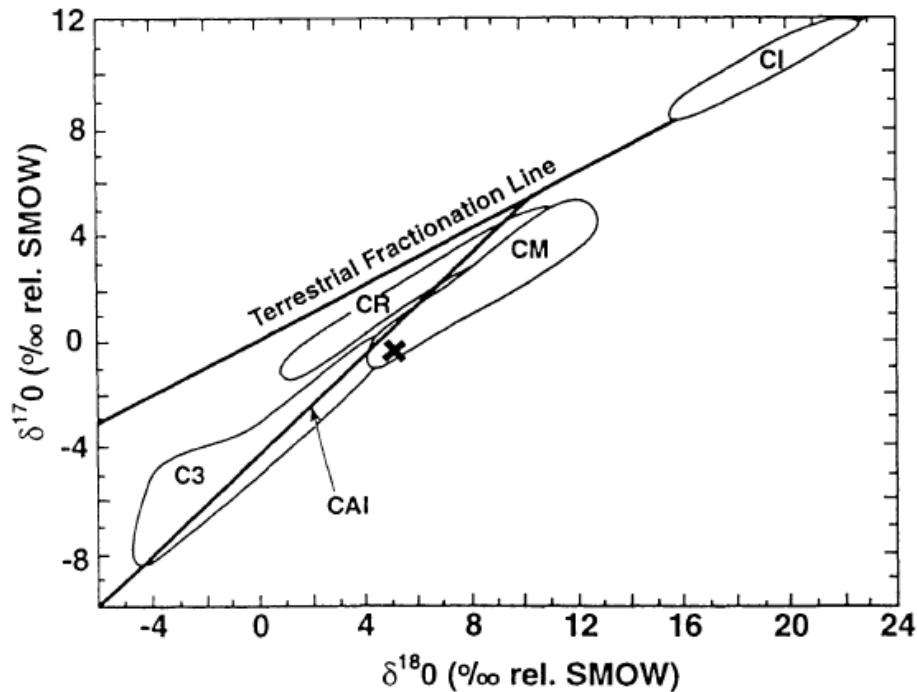


Figure 32: Oxygen isotope diagram comparing EET 87513, clast N (marked by the "x"), and different chondritic oxygen reservoirs (C3, CR, CM, and CI) relative to the terrestrial fractionation and refractory inclusion (CAI) lines. Thus, oxygen isotopes reveal that clast N is a CM chondrite. From Buchanan et al (1993b).

Based on this TL data, Sears et al (1991) paired the three meteorites together, along with EET 87509 and EET 87510, which were later excluded from the group by the work of Buchanan et al (2000). Interestingly, though EET 87531 was considered as a separate fall by Sears et al (1991), Sears et al (1997) later evaluated it as a prospective pair of EET 87509 and EET 87513, while noting that the pairing was

disputed by the work of Mittlefehldt and Lindstrom (1991a). The TL sensitivities reported by Sears et al (1997) for EET 87513 are within the range established by clast and matrix samples for the three

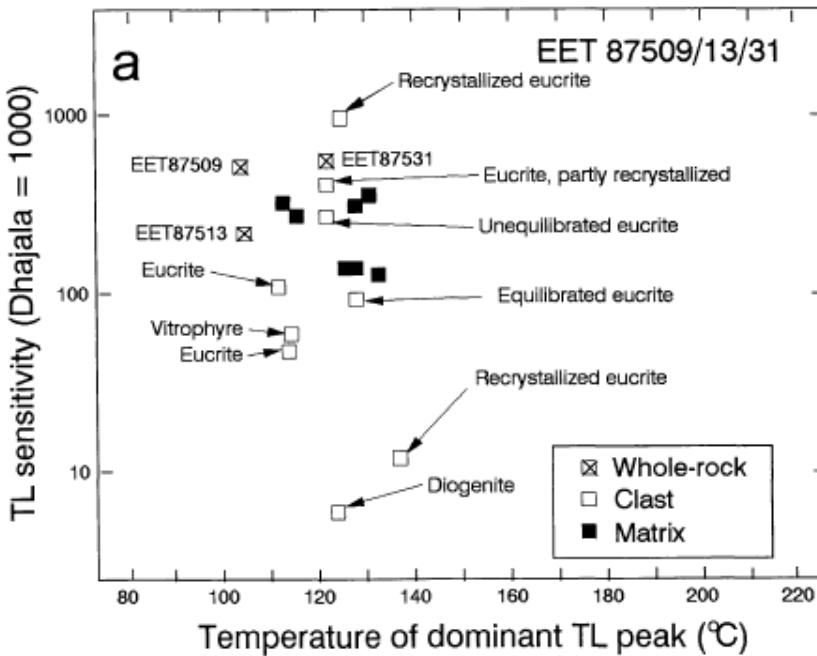


Figure 33: Peak TL sensitivity plotted against the temperatures at which those peaks were achieved, for clasts from EET 87509, 87513, and 87531. EET 87531 establishes both a minimum and maximum TL sensitivity for the group, perhaps reflective of the wider variety of clasts (i.e., EET 87513 is a howardite but EET 87509 and EET 87531 are polymict eucrites). From Sears et al (1997).

meteorites (EET 87509, EET 87513, EET 87531), but have slightly lower magnitude peak TL sensitivities which occur at generally higher temperatures than the other two meteorites. In addition, EET 87513 contains clastic material that establishes both high and low TL sensitivity outliers for the three meteorites (Sears et al, 1997; **Figure 33**), which may be reflective of the greater petrographic and mineralogical diversity of the EET 87513 howardite relative to the EET 87509 and EET 87531 polymict eucrites.

Natural remnant magnetism was investigated in EET 87503 by Collinson and Morden (1994); they found evidence of both primary and secondary NRM (**Figure 34**). They also observed that initial NRM directions were clustered, but scattered and diverged upon demagnetization, indicating that the components of the meteorite were partially remagnetized after meteorite assembly (Collinson and Morden, 1994), possibly due to the shock lithification cited by Metzler et al (1995). Additional magnetic work on EET 87503 was published by Gattacceca et al (2005), with a reported anisotropy of magnetic susceptibility (AMS) degree (P) of 1.829 and AMS shape parameter (T) of 0.21.

The reflectance spectrum of EET 87503 was first determined by Hiroi et al (1994), who found that the <25 μm size fraction of a sieved EET 87503 powder was a striking match with the reflectance spectrum and albedo of 4 Vesta (**Figure 35**), suggesting that the regolith of Vesta may contain similar proportions of diogenite and eucrite material to EET 87503 (Buchanan and Mittlefehldt, 2003). Hiroi et al (1995) noted that the Vesta spectrum determined by Binzel and Xu (1993) was slightly different from EET 87503, but attributed this dissimilarity to surface heterogeneity, a feature of Vesta observed by other spectral studies (e.g., Binzel et al, 1997; Gaffey, 1997). Additional spectral data for EET 87503 can be found in Hiroi and Pieters (1998), Burbine et al (2001), Pieters et al (2005), and Rivkin et al (2006).

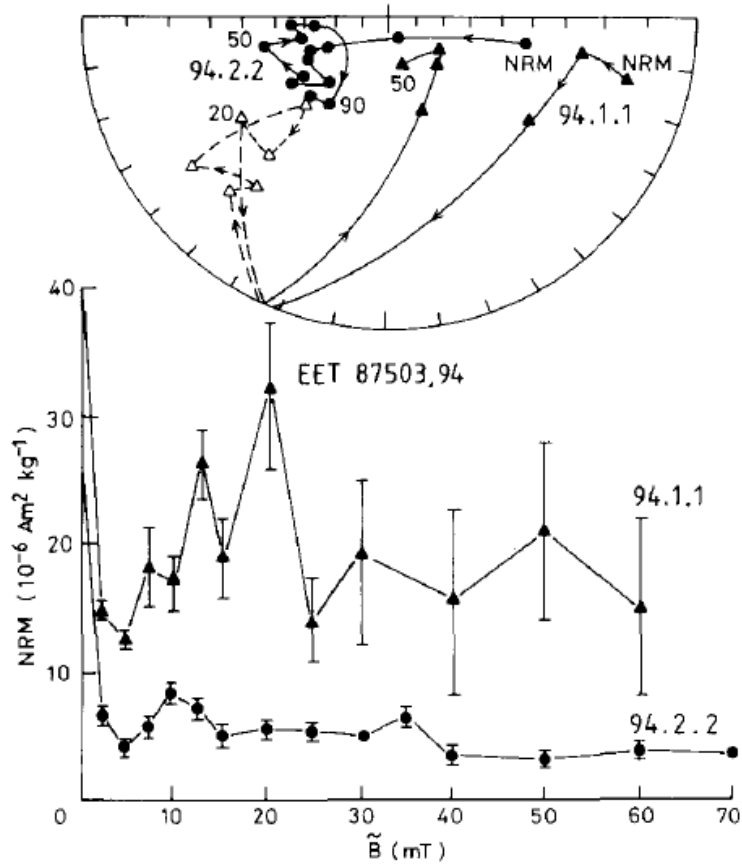


Figure 34: Alternating field demagnetization for two subsamples of EET 87503. Note that initial NRM directions are clustered but diverge upon demagnetization (see top), indicating partial remagnetization after meteorite assembly. From Collinson and Morden (1994).

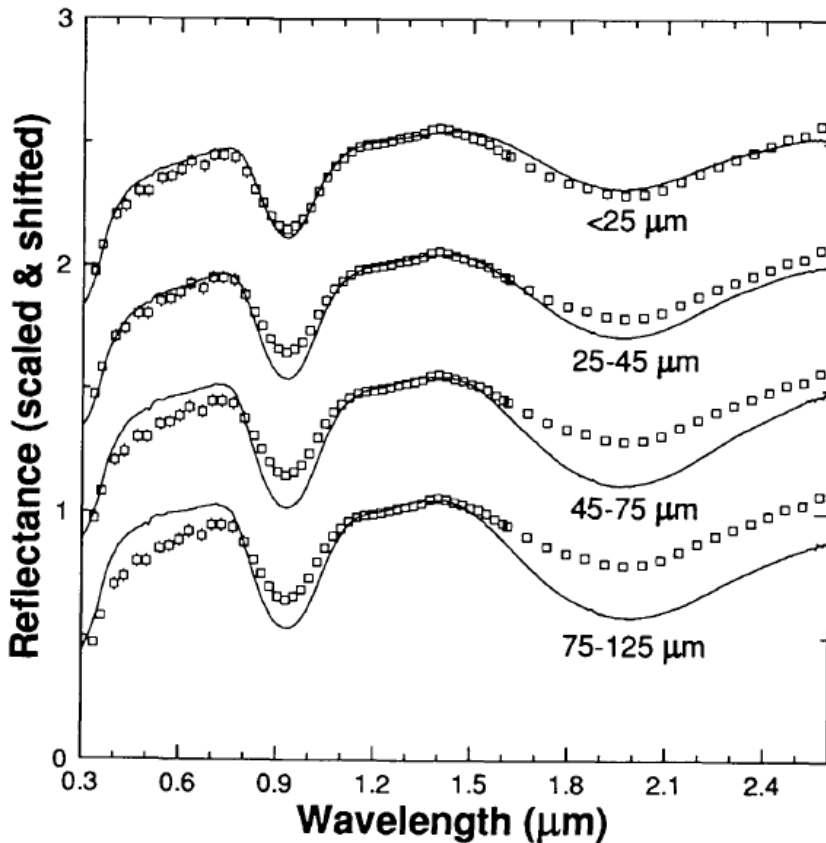


Figure 35: Comparison of reflectance spectra of Vesta (squares) and size-discriminated powders of EET 87503. The $<25 \mu\text{m}$ size fraction is a striking match to the asteroid, suggesting that the regolith may be composed of similar materials (in similar abundances) to the howardite. From Hiroi et al (1994).

Metamorphism: EET 87503 and EET 87513 contain a wide variety of equilibrated and unequilibrated clasts (e.g., Buchanan and Mittlefehldt, 2003), in addition to impact melt breccias (e.g., Metzler et al, 1995), suggesting a complicated metamorphic and impact history for these howardites. As a unique example, one clast from EET 87503 (sample ,63) contains a fine-grained, subophitic, quenched impact melt with equilibrated groundmass pyroxenes that contain augite exsolution lamellae, indicating a thermal metamorphic overprint on a sample that had clearly already experienced impact brecciation (Metzler et al, 1995). A possible metamorphic and impact history for EET87503 suggests initial crystallization of all components was followed by brecciation, a period of thermal metamorphism, and a second brecciation event (Metzler et al, 1995); the lack of matrix recrystallization and the preservation of a trapped solar gas component (Metzler et al, 1995) indicate minimal metamorphism after final aggregation (Buchanan, 1995; Buchanan and Mittlefehldt, 2003).

Shock and Impact Effects: Many of the clasts described above have shocked, blackened pyroxenes (Buchanan, 1995; Buchanan and Lindstrom, 2000; Buchanan, 2002; Buchanan and Mittlefehldt, 2003); the conclusion that they were shocked is consistent with other textural observations such as undulose extinction and incipient mosaicism (Buchanan and Mittlefehldt, 2003). Many clasts show evidence of impact melting or impact brecciation, especially ones that consist of silicate fragments in a black, glassy matrix (Buchanan and Mittlefehldt, 2003). Metzler et al (1995) also noted that the matrix of EET 87503 is apparently densely shock-lithified but not recrystallized.

Terrestrial Weathering: Mittlefehldt and Lindstrom (1991a) reported on the effect of terrestrial weathering on REE by analyzing two different samples from EET 87503 (samples ,23 and ,53). Whereas EET 87503,23 exhibited no obvious weathering effects on the exterior, an interior sample showed a slight negative Ce anomaly; the opposite was true for EET 87503,53, which showed no REE weathering effects on an interior sample, but depleted LREE and a negative Ce anomaly on an exterior sample (Mittlefehldt and Lindstrom, 1991a). However, later analyses by D. Mittlefehldt (published in Wang et al, 1992) generally suggested that EET 87503 experienced LREE weathering enrichment in its interior, excepting Ce, resulting in an exterior/interior ratio for Ce of 1.1. Labile trace elements (such as Ag, Au, Co, Ga, In, Sb, and Tl) were apparently unaffected by the same process and are not enriched in one set of samples compared to the other, perhaps reflecting greater dispersion of these elements among different phases (Wang et al, 1992). Finally, though there is clear evidence concerning the effects of terrestrial weathering on EET 87503, most clasts in EET 87503 and EET 87513 appear to lack any significant chemical signature of such weathering (Buchanan and Mittlefehldt, 2003)

Processing: Summaries of the processing and allocation history for both EET 87503 and EET 87513 are shown below in **Tables 8** and **9**, with a listing of clasts for EET 87513 in **Table 10**. Photos of the main mass of EET 87513 and subdivision into pieces revealing many clasts are shown in **Figure 36 to 41**. For EET 87503 ten clasts were identified and are located in **Figures 42 to 44**.

Table 8: Processing and allocation history of EET 87503, courtesy of K. Righter at NASA-JSC. This table is current as of 08/20/2009.

Sample	Parent	Location	Mass	Description
EET 87503,0	0	MPL (Houston)	293.800	E Butt
EET 87503,1	0	Consumed	2.420	Potted Butt
EET 87503,2	1	Mason, B./NSF	0.010	PM
EET 87503,3	0	Sears, D.W.G./NSF	0.300	TL Chip/Interior Piece
EET 87503,4	0	MPL (Houston)	26.883	LOC Chips
EET 87503,6	1	Mittlefehldt, D.W.	0.010	PM
EET 87503,7	1	MCC (Houston)	0.010	PM
EET 87503,8	1	MCC (Houston)	0.010	PM
EET 87503,9	1	Delaney, J.S.	0.010	PM
EET 87503,10	0	Jarosewich, E./NSF	30.280	Interior Chips
EET 87503,11	0	Lipschutz, M.E.	0.460	Interior Chip
EET 87503,12	0	Gibson, E.K.	2.090	Interior Chip
EET 87503,13	0	Shaw, D.	1.080	Interior Chip
EET 87503,14	0	Sears, D.W.G.	0.350	Interior Chip
EET 87503,15	0	MPL (Houston)	10.390	Chips + FI
EET87503, 17	1	Lost in the Mail	0.010	PM
EET87503, 18	0	MPL (Houston)	37.176	BS FI
EET87503, 19	0	Entirely Subdivided	--	--
EET87503, 20	0	MPL (Houston)	29.527	Chips + FI
EET87503, 21	0	NMNH/Smithsonian	662.500	W Butt
EET87503, 23	19	Mittlefehldt, D.W.	1.557	Grey Clast #2
EET87503, 24	19	Mittlefehldt, D.W.	0.940	Matrix Chip
EET87503, 25	19	Mittlefehldt, D.W.	0.223	Eucrite Clast
EET87503, 26	19	Mittlefehldt, D.W.	0.068	Eucrite Clast #7
EET87503, 27	19	Mittlefehldt, D.W.	0.081	Eucrite Clast
EET87503, 28	19	MPL (Houston)	5.653	Int/Ext LOC Chips
EET87503, 29	19	MPL (Houston)	2.477	Documented Chip
EET87503, 30	19	MPL (Houston)	1.158	Documented Interior Chip
EET87503, 31	19	MPL (Houston)	4.159	Documented Chip
EET87503, 32	19	MPL (Houston)	4.396	Documented Chip
EET87503, 33	19	MPL (Houston)	13.942	Slab Pieces
EET87503, 34	19	MPL (Houston)	14.911	Chips + FI
EET87503, 35	19	Mittlefehldt, D.W.	0.066	Dark Clast #6
EET87503, 36	19	MPL (Houston)	1.447	Interior Chips
EET87503, 37	19	MPL (Houston)	7.605	Documented Slab
EET87503, 38	19	Mittlefehldt, D.W.	0.718	Green Clast #5
EET87503, 39	19	MPL (Houston)	11.297	Documented Slab
EET87503, 40	19	MPL (Houston)	4.312	Documented Slab
EET87503, 41	19	MPL (Houston)	5.360	Documented Slab
EET87503, 42	19	Mittlefehldt, D.W.	0.390	Eucrite Clast + Matrix #9
EET87503, 43	19	MPL (Houston)	6.711	Documented Slab
EET87503, 44	19	MPL (Houston)	6.653	Documented Slab
EET87503, 45	19	MPL (Houston)	3.072	Documented Slab
EET87503, 46	19	Mittlefehldt, D.W.	0.312	Unusual Clast #10
EET87503, 47	19	MPL (Houston)	5.869	Documented Slab
EET87503, 48	19	MPL (Houston)	1.456	Documented Interior Chip

Table 8 (cont.): Processing and allocation history of EET 87503, courtesy of K. Righter at NASA-JSC. This table is current as of 08/20/2009.

EET87503, 49	19	MPL (Houston)	2.167	Documented Slab
EET87503, 50	19	MPL (Houston)	8.269	Documented Slab
EET87503, 51	19	MPL (Houston)	6.805	Chips + FI
EET87503, 53	20	Mittlefehldt, D.W.	3.474	Eucrite Clast #1
EET87503, 54	20	Mittlefehldt, D.W.	0.618	Fusion Crust
EET87503, 55	20	MPL (Houston)	6.010	Documented Chip
EET87503, 56	20	MPL (Houston)	13.019	Documented Chip
EET87503, 58	0	MPL (Houston)	9.905	Chips + FI
EET87503, 59	0	MPL (Houston)	1.663	Chips + FI
EET87503, 60	0	MPL (Houston)	13.872	BS FI
EET87503, 62	58	MRS (Houston)	1.059	Chips + PIPM
EET87503, 63	58	MRS (Houston)	1.150	Chips + PIPM
EET87503, 64	58	MRS (Houston)	2.262	Chips + PIPM
EET87503, 65	58	MRS (Houston)	0.930	Chip + 2 PIPM
EET87503, 66	58	MRS (Houston)	0.436	Chip + 2 PIPM
EET87503, 67	58	MRS (Houston)	1.113	Chip
EET87503, 68	58	MRS (Houston)	0.238	Chip + PIPM
EET87503, 69	58	MRS (Houston)	0.541	Chip + PIPM
EET87503, 70	58	MRS (Houston)	0.817	Chip
EET87503, 71	58	MPL (Houston)	0.218	Chip
EET87503, 72	58	MPL (Houston)	0.362	Clast
EET87503, 73	58	MPL (Houston)	11.094	Documented Piece
EET87503, 74	58	MPL (Houston)	6.836	Documented Piece
EET87503, 75	58	MPL (Houston)	8.596	Documented Piece
EET87503, 76	58	MPL (Houston)	4.834	Documented Piece
EET87503, 77	58	MPL (Houston)	20.680	Documented Piece
EET87503, 78	58	MPL (Houston)	16.534	Documented Piece
EET87503, 79	58	MPL (Houston)	8.519	Documented Piece
EET87503, 80	58	MPL (Houston)	6.622	Documented Piece
EET87503, 81	58	MPL (Houston)	25.136	Documented Piece
EET87503, 82	58	MPL (Houston)	2.129	Documented Piece
EET87503, 83	58	MPL (Houston)	5.433	Documented Piece
EET87503, 84	58	MPL (Houston)	3.645	Documented Piece
EET87503, 85	58	MPL (Houston)	4.457	Documented Piece
EET87503, 86	58	MPL (Houston)	1.429	Documented Pieces
EET87503, 87	58	MPL (Houston)	2.248	Documented Pieces
EET87503, 88	58	MPL (Houston)	8.437	Interior Chips
EET87503, 89	0	MPL (Houston)	54.192	Documented Piece
EET87503, 90	0	MPL (Houston)	30.383	LOC Pieces
EET87503, 91	0	MPL (Houston)	38.393	Exterior Pieces
EET87503, 92	0	MPL (Houston)	24.519	Interior Chips
EET87503, 93	0	MPL (Houston)	10.876	Chips + FI
EET87503, 94	0	Collinson, D.W.	10.428	Interior Chip
EET87503, 95	0	Thiemens, M.H.	1.193	Interior Chip
EET87503, 97	90	Hiroi, T.	10.592	Interior Chip
EET87503, 98	90	MPL (Houston)	10.535	Interior Chips + FI
EET87503, 99	90	MPL (Houston)	3.749	Chips + FI

Table 8 (cont.): Processing and allocation history of EET 87503, courtesy of K. Righter at NASA-JSC. This table is current as of 08/20/2009.

EET87503, 100	30	Domeneghetti, M.C.	0.110	Interior Chip
EET87503, 101	34	MCC (Houston)	0.583	Clast Q, Potted Butt
EET87503, 102	34	MCC (Houston)	0.562	Clast R, Potted Butt
EET87503, 103	34	MPL (Houston)	2.595	Chips + FI
EET87503, 105	33	Buchanan, P.C.	0.051	Clast M
EET87503, 106	33	Buchanan, P.C.	0.183	Clast M
EET87503, 107	33	MCC (Houston)	0.341	Clast M, Potted Butt
EET87503, 108	33	MCC (Houston)	1.852	Clast N, Potted Butt
EET87503, 109	33	Buchanan, P.C.	0.069	Clast L
EET87503, 110	33	MCC (Houston)	0.283	Clast L, Potted Butt
EET87503, 111	33	MPL (Houston)	12.677	Chips + FI
EET87503, 113	91	MCC (Houston)	1.557	Clast Z, Potted Butt
EET87503, 114	91	MPL (Houston)	1.587	Chips + FI
EET87503, 116	92	Buchanan, P.C.	0.258	Clast Z
EET87503, 118	81	MCC (Houston)	1.827	Clast H, Potted Butt
EET87503, 119	81	MCC (Houston)	0.185	Clast J, Potted Butt
EET87503, 120	81	MPL (Houston)	2.206	Chips + FI
EET87503, 122	78	Buchanan, P.C.	0.121	Clast BA
EET87503, 123	78	MCC (Houston)	0.796	Clast BA, Potted Butt
EET87503, 124	78	MCC (Houston)	1.083	Clast BB, Potted Butt
EET87503, 125	78	MPL (Houston)	1.909	Chips + FI
EET87503, 127	4	MCC (Houston)	1.291	Clast BC, Potted Butt
EET87503, 129	0	MCC (Houston)	1.709	Clast B, Potted Butt
EET87503, 130	0	Entirely Subdivided	--	--
EET87503, 131	0	MPL (Houston)	13.300	Chips, S Face
EET87503, 132	0	MCC (Houston)	0.367	Clast D, Potted Butt
EET87503, 133	0	MPL (Houston)	7.596	LOC Chip
EET87503, 134	0	MCC (Houston)	0.438	Clast E, Potted Butt
EET87503, 135	0	MCC (Houston)	1.622	Clast F, Potted Butt
EET87503, 136	0	Buchanan, P.C.	0.084	Clast F
EET87503, 137	0	MPL (Houston)	5.958	LOC Chips
EET87503, 138	0	MPL (Houston)	16.908	Chips + FI
EET87503, 140	137	Binzel, R.P.	4.140	2 LOC Chips
EET87503, 141	101	Consumed	0.010	THK. PM
EET87503, 142	102	MCC (Houston)	0.010	THK. PM
EET87503, 143	107	MCC (Houston)	0.010	THK. PM
EET87503, 144	108	MCC (Houston)	0.010	THK. PM
EET87503, 145	110	Consumed	0.010	THK. PM
EET87503, 146	113	Consumed	0.010	THK. PM
EET87503, 147	118	MCC (Houston)	0.010	THK. PM
EET87503, 148	119	MCC (Houston)	0.010	THK. PM
EET87503, 149	123	Consumed	0.010	THK. PM
EET87503, 150	124	MCC (Houston)	0.010	THK. PM
EET87503, 151	127	MCC (Houston)	0.010	THK. PM
EET87503, 152	129	MCC (Houston)	0.010	THK. PM
EET87503, 153	130	MCC (Houston)	0.010	THK. PM
EET87503, 155	132	MCC (Houston)	0.010	THK. PM

Table 8 (cont.): Processing and allocation history of EET 87503, courtesy of K. Righter at NASA-JSC. This table is current as of 08/20/2009.

EET87503, 156	134	MCC (Houston)	0.010	THK. PM
EET87503, 157	135	Lee, C.	0.010	THK. PM
EET87503, 158	131	Bunch, T.	5.132	Exterior Chip, S Face
EET87503, 160	88	Buchanan, P.C.	0.227	Interior Chip
EET87503, 162	92	Buchanan, P.C.	0.229	Interior Chip
EET87503, 164	20	Lee, D.	8.096	Interior Chips
EET87503, 166	131	Mittlefehldt, D.W.	5.460	Interior Chips
EET87503, 168	88	Ebihara, M.	5.057	Interior Chips
EET87503, 170	36	Moynier, F.	0.721	Interior Chips

Table 9: Processing and allocation history of EET 87513, courtesy of K. Righter at NASA-JSC. This table is current as of 08/20/2009.

Sample	Parent	Location	Mass (g)	Description
EET 87513,0	0	MPL (Houston)	114.484	--
EET 87513,1	0	MPL (Houston)	11.390	Documented Chip
EET 87513,2	0	Sears, D.W.G./NSF	0.500	TL Chip/Interior Chip
EET 87513,3	0	MCC (Houston)	1.500	Potted Butt
EET 87513,4	0	MPL (Houston)	4.389	LOC Chip
EET 87513,5	0	MPL (Houston)	5.760	LOC Chip
EET 87513,6	0	MPL (Houston)	4.240	Chips + FI
EET 87513,7	3	Mittlefehldt, D.W.	0.010	PM
EET 87513,8	3	Mason, B.H./NSF	0.010	PM
EET 87513,9	1	Gibson, E.K.	2.520	Interior Chip
EET 87513,10	0	MPL (Houston)	44.400	2 Documented Pieces
EET 87513,11	0	MPL (Houston)	20.105	Chips + FI
EET 87513,12	0	MPL (Houston)	18.512	Chips + FI
EET 87513,13	0	MPL (Houston)	16.118	Documented Piece
EET 87513,14	0	MPL (Houston)	18.420	Documented Piece
EET 87513,15	0	MPL (Houston)	1.349	Chips + FI
EET 87513,16	0	MPL (Houston)	11.499	BS FI
EET 87513,17	0	MPL (Houston)	3.085	Chips
EET 87513,18	0	Nyquist, L.E.	0.235	Clast E Chips
EET 87513,19	0	MPL (Houston)	0.023	Clast E + Matrix Chip
EET 87513,20	0	MPL (Houston)	0.035	Clast E + Matrix Chip
EET 87513,21	0	MCC (Houston)	0.463	Potted Butt
EET 87513,22	0	MCC (Houston)	0.081	Potted Butt
EET 87513,23	0	Schmitt, R.A.	0.042	Clast A Chips
EET 87513,24	0	MCC (Houston)	0.013	Potted Butt
EET 87513,25	0	Schmitt, R.A.	0.044	Clast B Chip
EET 87513,26	0	MCC (Houston)	0.007	PM
EET 87513,27	0	Mittlefehldt, D.W.	0.007	Clast C Chip
EET 87513,28	0	MCC (Houston)	0.005	PM
EET 87513,29	0	MPL (Houston)	0.008	Chip with Black Clast
EET 87513,30	0	MPL (Houston)	0.370	Matrix Chips
EET 87513,31	0	MCC (Houston)	0.202	Potted Butt
EET 87513,32	0	Mittlefehldt, D.W.	0.012	Clast T Chips
EET 87513,33	0	MCC (Houston)	0.008	PM
EET 87513,34	0	MCC (Houston)	0.002	Potted Butt
EET 87513,35	0	Schmitt, R.A.	0.063	Clast Y Chips
EET 87513,36	0	MPL (Houston)	0.064	Clast Y + Matrix Chips
EET 87513,37	0	MCC (Houston)	0.126	Potted Butt
EET 87513,38	0	Mittlefehldt, D.W.	0.070	Clast P Chip
EET 87513,39	0	MPL (Houston)	0.057	Clast P + Matrix Chips
EET 87513,40	0	MCC (Houston)	0.025	Potted Butt
EET 87513,41	0	Schmitt, R.A.	0.025	Clast N Chips
EET 87513,42	0	MCC (Houston)	0.021	Potted Butt
EET 87513,43	0	MPL (Houston)	0.026	Clast N + Matrix Chips
EET 87513,44	0	MPL (Houston)	0.042	Chips with Clast N, Matrix
EET 87513,45	0	MPL (Houston)	0.012	Clast EE Chips
EET 87513,46	0	MCC (Houston)	0.011	Potted Butt
EET 87513,47	0	MCC (Houston)	0.724	Potted Butt
EET 87513,48	0	Mittlefehldt, D.W.	0.264	Matrix Chips
EET 87513,49	0	MPL (Houston)	0.508	Matrix Chips
EET 87513,50	0	Mittlefehldt, D.W.	0.151	Matrix Chip

EET 87513,51	0	MCC (Houston)	1.627	Potted Butt
EET 87513,52	0	MPL (Houston)	1.438	Documented Exterior Chip
EET 87513,53	0	MPL (Houston)	2.275	Chips + FI
EET 87513,54	0	MPL (Houston)	2.721	Exterior Chip
EET 87513,55	0	MPL (Houston)	1.498	3 Interior Matrix Chips
EET 87513,56	0	Mittlefehldt, D.W.	0.165	2 Matrix Chips
EET 87513,57	0	MPL (Houston)	1.387	Matrix Chip with Fusion Crust
EET 87513,58	0	MPL (Houston)	3.957	Chips + FI
EET 87513,59	0	MPL (Houston)	3.979	Chips + FI
EET 87513,61	24	MCC (Houston)	0.010	PM
EET 87513,62	34	MCC (Houston)	0.010	PM
EET 87513,63	40	MCC (Houston)	0.010	PM
EET 87513,64	42	Reid, A.M.	0.010	PM
EET 87513,65	46	MCC (Houston)	0.010	PM
EET 87513,66	59	MRS (Houston)	0.002	Dark Fragments
EET 87513,67	58	MRS (Houston)	0.002	Dark Fragments
EET 87513,69	37	MCC (Houston)	0.010	PM
EET 87513,70	31	MCC (Houston)	0.010	PM
EET 87513,71	51	MCC (Houston)	0.010	PM
EET 87513,72	47	MCC (Houston)	0.010	PM
EET 87513,73	21	MCC (Houston)	0.010	PM
EET 87513,74	22	MCC (Houston)	0.010	PM
EET 87513,75	25	MPL (Houston)	0.036	Clast B Chips
EET 87513,76	18	Schmitt, R.A.	0.038	Clast E Chips
EET 87513,77	18	Mittlefehldt, D.W.	0.039	Clast E Chips
EET 87513,78	18	Sears, D.W.G.	0.026	Clast E Chips
EET 87513,79	18	Clayton, R.N.	0.012	Clast E Chips
EET 87513,80	32	Sears, D.W.G.	0.009	Clast T Chips
EET 87513,81	35	Sears, D.W.G.	0.021	Clast Y
EET 87513,82	38	Nyquist, L.E.	0.040	Clast P Chips
EET 87513,83	38	Clayton, R.N.	0.013	Clast P Chips
EET 87513,84	41	Clayton, R.N.	0.011	Clast N Chips
EET 87513,85	45	Sears, D.W.G.	0.012	Clast EE Chips
EET 87513,86	30	Mittlefehldt, D.W.	0.151	Matrix Chip
EET 87513,87	30	Swindle, T.D.	0.167	Matrix Chip
EET 87513,88	56	Lipschutz, M.E.	0.158	Matrix Chips
EET 87513,89	56	Nyquist, L.E.	0.166	Matrix Chips
EET 87513,90	56	Swindle, T.D.	0.154	Matrix Chips
EET 87513,91	56	Sears, D.W.G.	0.111	Matrix Chips
EET 87513,92	56	Clayton, R.N.	0.034	Matrix Chips
EET 87513,93	50	Lipschutz, M.E.	0.145	Matrix Chips
EET 87513,94	50	Nyquist, L.E.	0.140	Matrix Chips
EET 87513,95	50	Swindle, T.D.	0.141	Matrix Chips
EET 87513,96	50	Sears, D.W.G.	0.104	Matrix Chip
EET 87513,97	50	Clayton, R.N.	0.032	Matrix Chip
EET 87513,98	48	Lipschutz, M.E.	0.161	Matrix Chip

Table 9 (cont.): Processing and allocation history of EET 87513, courtesy of K. Righter at NASA-JSC. This table is current as of 08/20/2009.

EET 87513,99	48	Swindle, T.D.	0.169	Matrix Chips
EET 87513,100	48	Sears, D.W.G.	0.106	Matrix Chips
EET 87513,101	49	Mittlefehldt, D.W.	0.287	Matrix Chips
EET 87513,102	53	Mittlefehldt, D.W.	0.362	2 Exterior Chips
EET 87513,103	21	MCC (Houston)	0.010	PM
EET 87513,104	44	Domeneghetti, M.C.	0.110	Interior Chip
EET 87513,105	59	Hiroi, T.	0.155	Chip
EET 87513,107	0	MCC (Houston)	1.415	Clast 6, Potted Butt
EET 87513,108	0	MCC (Houston)	0.972	Clast 5, Potted Butt
EET 87513,109	0	Buchanan, P.	0.097	Clast 5
EET 87513,110	0	MPL (Houston)	18.758	LOC Chips
EET 87513,111	0	MPL (Houston)	6.250	Chips + FI
EET 87513,113	10	MCC (Houston)	0.535	Clast E, Potted Butt
EET 87513,114	10	MPL (Houston)	4.385	Clast E
EET 87513,115	10	MPL (Houston)	6.038	Chips
EET 87513,117	4	MCC (Houston)	0.010	Clast 7, Potted Butt
EET 87513,118	4	Buchanan, P.	0.071	Clast 7
EET 87513,119	10	MCC (Houston)	0.794	Clast 8, Potted Butt
EET 87513,120	10	MCC (Houston)	1.235	Clast 9, Potted Butt
EET 87513,121	10	MPL (Houston)	1.128	Chips + FI
EET 87513,123	107	MCC (Houston)	0.010	THK. PM
EET 87513,124	108	MCC (Houston)	0.010	THK. PM
EET 87513,125	113	MCC (Houston)	0.010	THK. PM
EET 87513,126	117	MCC (Houston)	0.010	THK. PM
EET 87513,127	119	MCC (Houston)	0.010	THK. PM
EET 87513,128	120	MCC (Houston)	0.010	THK. PM
EET 87513,129	55	Buchanan, P.	0.277	Interior Matrix Chip
EET 87513,131	120	MCC (Houston)	0.010	Thick
EET 87513,132	12	Lee, D.	10.103	2 Interior Chips
EET 87513,134	11	Mittlefehldt, D.W.	5.080	Interior Chips
EET 87513,136	10	Mittlefehldt, D.W.	5.620	Interior Chips
EET 87513,137	10	MPL (Houston)	22.500	Chips + FI
EET 87513,139	11	Ebihara, M.	2.064	Interior Chips

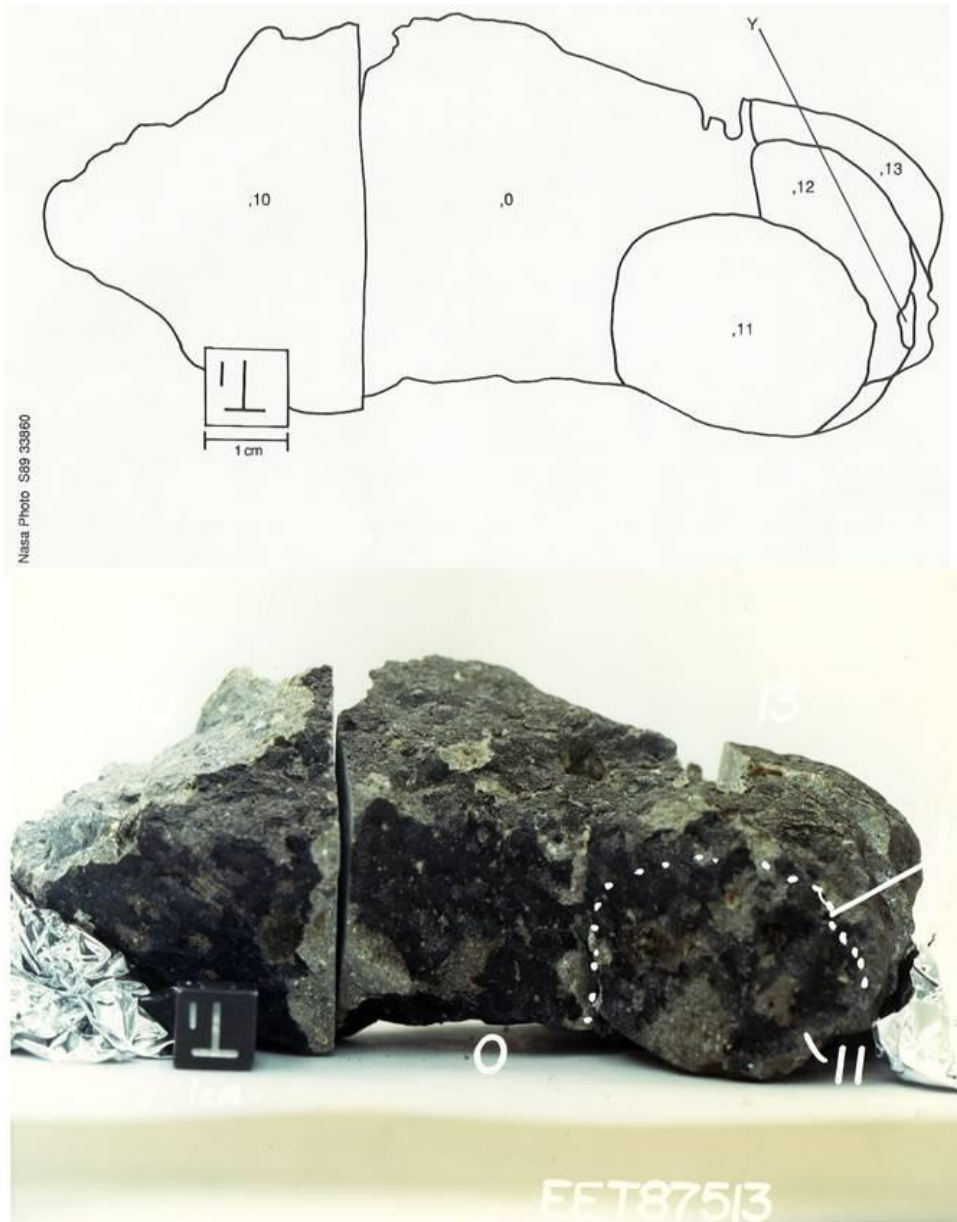


Figure 36: Photo and sketch of subdivision of EET 87513,0 into 0, 10, 11, 12 and 13.

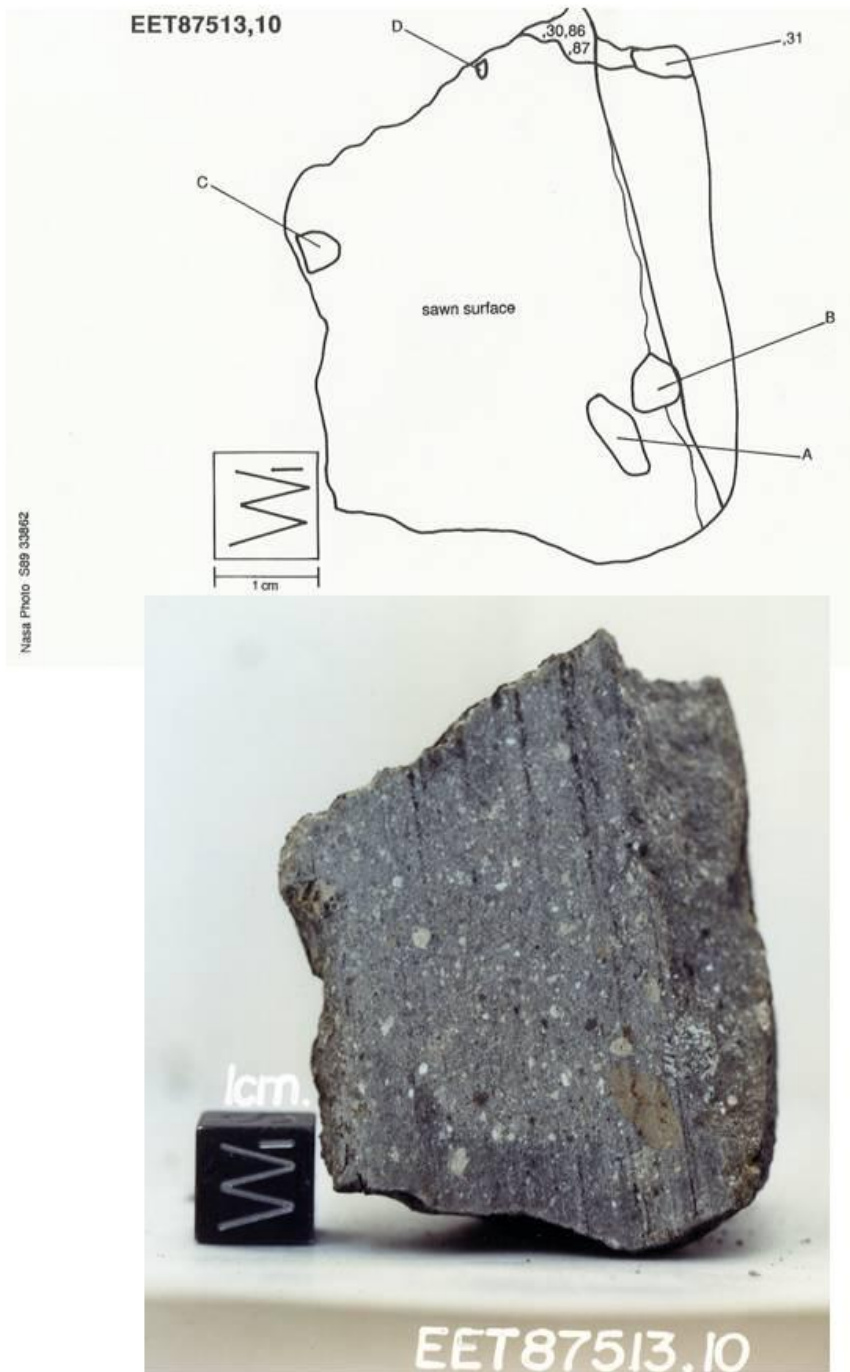
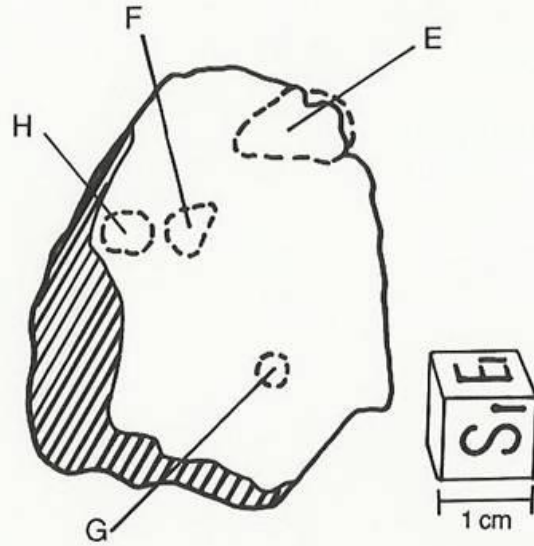


Figure 37: Photo and sketch of subdivision of EET 87513, 10 (West face) and locations of clasts A, B, C, and D.

EET87513,10



----- represents interior sample



Figure 38: Photo and sketch of subdivision of EET 87513, 10 (South Face) and locations of clasts E, F, G, and H.

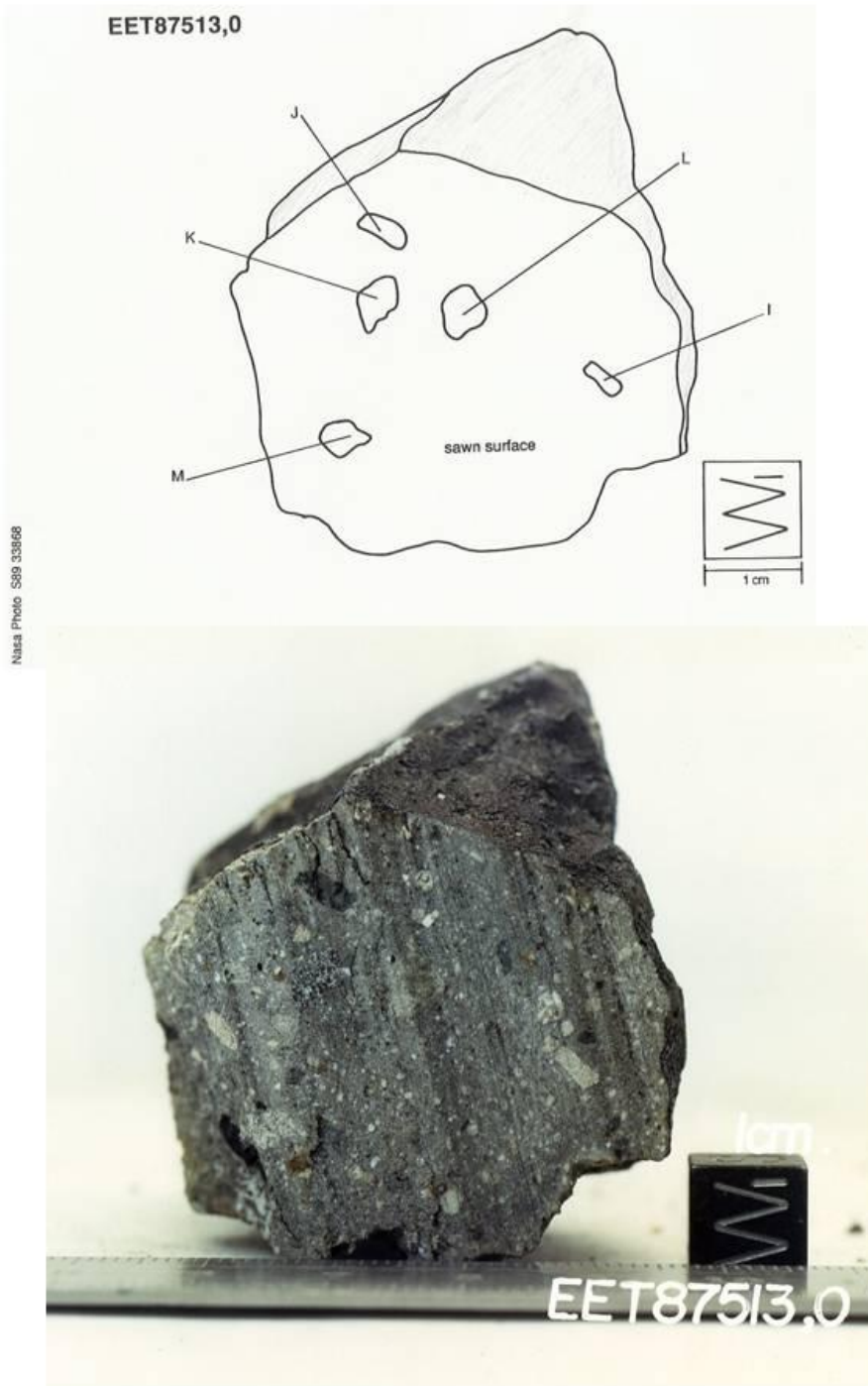


Figure 39: Photo and sketch of subdivision of EET 87513, 0 (West Face) and locations of clasts I, J, K, L, and M.

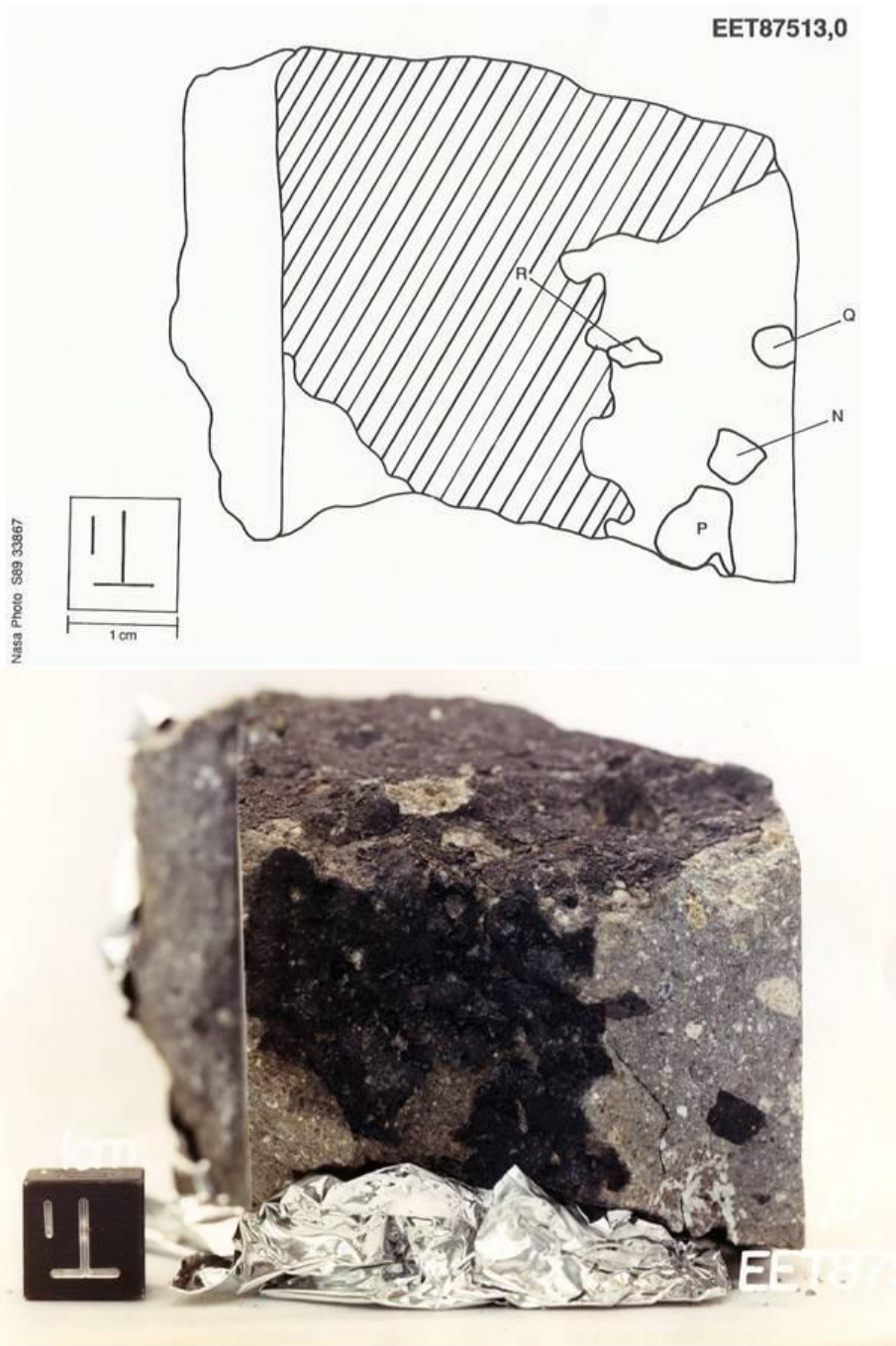


Figure 40: Photo and sketch of subdivision of EET 87513, 0 (West Face) and locations of clasts N, P, Q, and R.

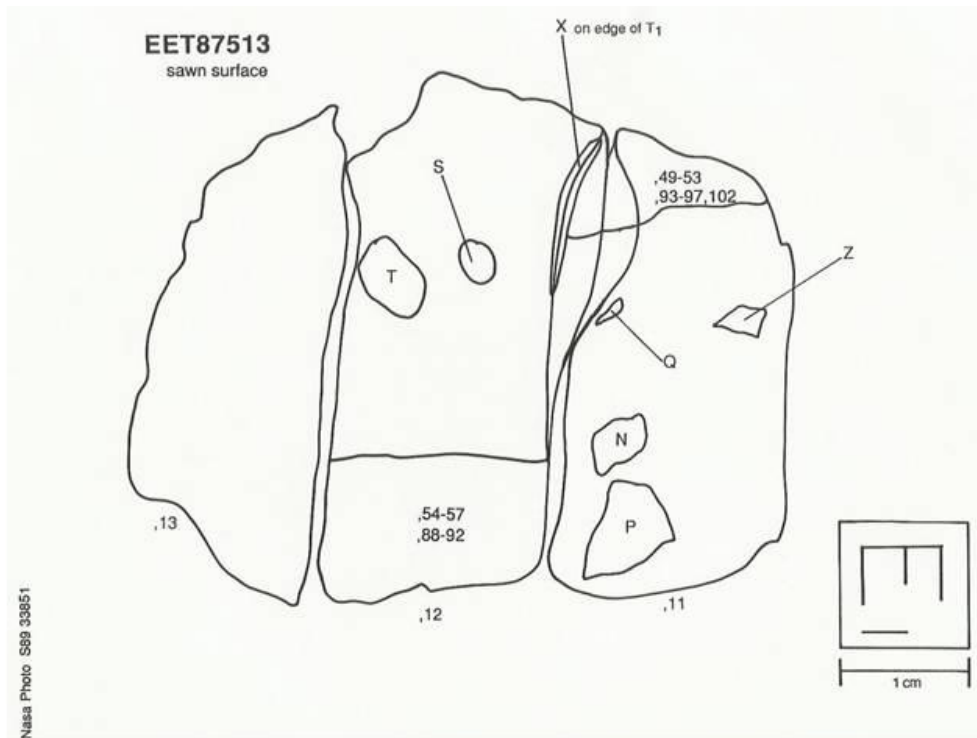


Figure 41: Photo and sketch of subdivision of EET 87513, 11, 12, and 13 and locations of clasts N, P, Q, S, T, X, and Z.

Table 10: Summary of clasts and descriptions from the curatorial notes for EET 87513.

SUMMARY OF EET87513 CLASTS:

CLAST	WEIGHT	TYPE
A	.042g	lt. brown, fi-grained, recrystallized diogenite (same clast as EE)
B	.08	euclite
C	.007	diogenite
E	.35	euclite
T	.021	diogenite
X	TS only	rusty px-rich euclite
Y	.084	euclite
P	.123	euclite
N	.036	black clast, carbonaceous; 5x3mm
EE	.024	recrystallized diogenite (same clast as A)
CC & DD	PTS only	fi-gr dk gray, black shiny, w/silicates

ALL CLASTS (as described by Arch Reid):

A	Brownish, pyroxene-rich clast; recrystallized diogenite; 8x4mm
B	Light gray euclite, igneous texture; 6x5mm
C	Coarse grained diogenite, on edge; 2x4mm
D	Very shiny, black, carbonaceous (?), 1x1mm
E	Medium grained euclite, adjacent to saw cut; 12x6mm
F	Dark gray, fine-grained, minor white silicates and a few rusty spots; 4x3mm
G	Green diogenite (?); 2x1.5mm
H	Euclite (?), black pyroxene around vug
I	Rectangular, fine-grained euclite; 4x1.5mm
J	Shiny, black rectangular with a few rust spots; 4.5x2mm
K	Euclite, medium grained, igneous texture; 4x3.5mm
L	Medium grained diogenite, rectangular shaped; 4x4mm
M	Fine-grained euclite, light colored; 3x2mm
N	Rectangular, shiny black clast with small amount silicates, carbonaceous; 5x3mm
P	Medium/coarse grained euclite adjacent to fusion crust; 6x8.5mm
Q	Fine-grained cinnamon colored euclite; 2.5x5mm
R	Dark, brown, pyroxene-rich (?), next to fusion crust; 4x1.5mm
S	Fine-grained euclite, igneous texture; 2x2.5mm
T	Green diogenite; 4x3mm
U	Fine-grained dark gray clast, few rusty spots; 2.5x3mm
V	Fine-grained dark gray, few rusty spots; 3x1.5mm
W	Fine-grained euclite; 4x3mm
X	Rusty, pyroxene-rich euclite; 4x3.5mm
Y	Exterior, medium/coarse grained euclite clast; 8x7mm
Z	Dark Brown; 4x1.5mm
AA	Polymict clast, dark gray with euclite(?) inclusion; 5x4mm
BB	Fine-grained euclite, igneous texture; ~3x4mm
CC	Fine-grained dark gray; 2x2mm
DD	Black shiny carbonaceous clast with minor silicates; 2x1mm
EE	Rusty, with black rim, probably px-rich, recrystallized diogenite; 3.5x1mm

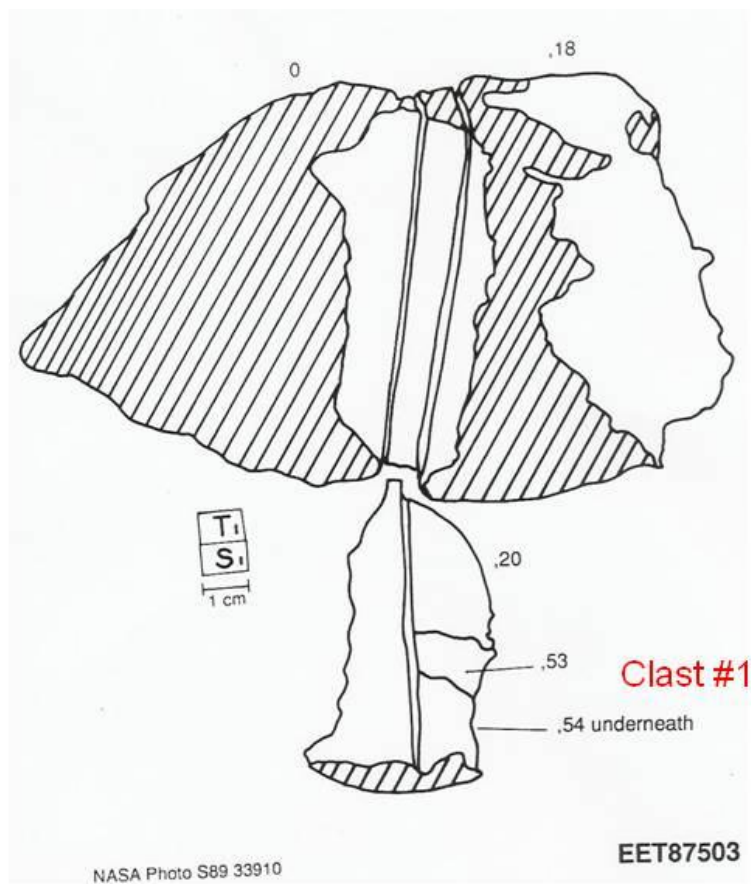


Figure 42: Location of clast #1 in EET 87503, exposed during cut of ,0 and ,18.

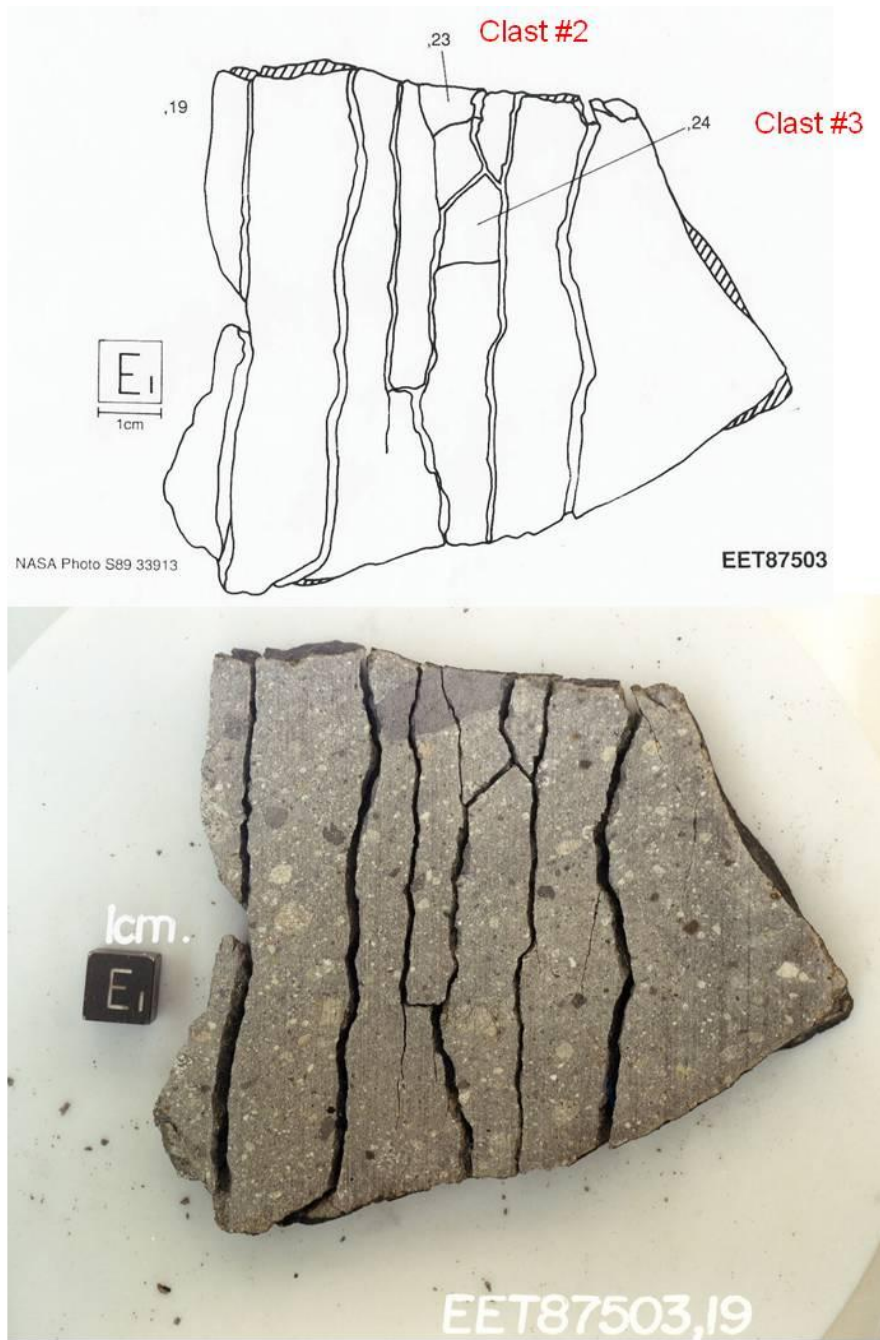


Figure 43: Location of clasts #2 and 3 exposed in E side of slab of EET 87503 (,19). These two clasts are splits ,23 and ,24, respectively.

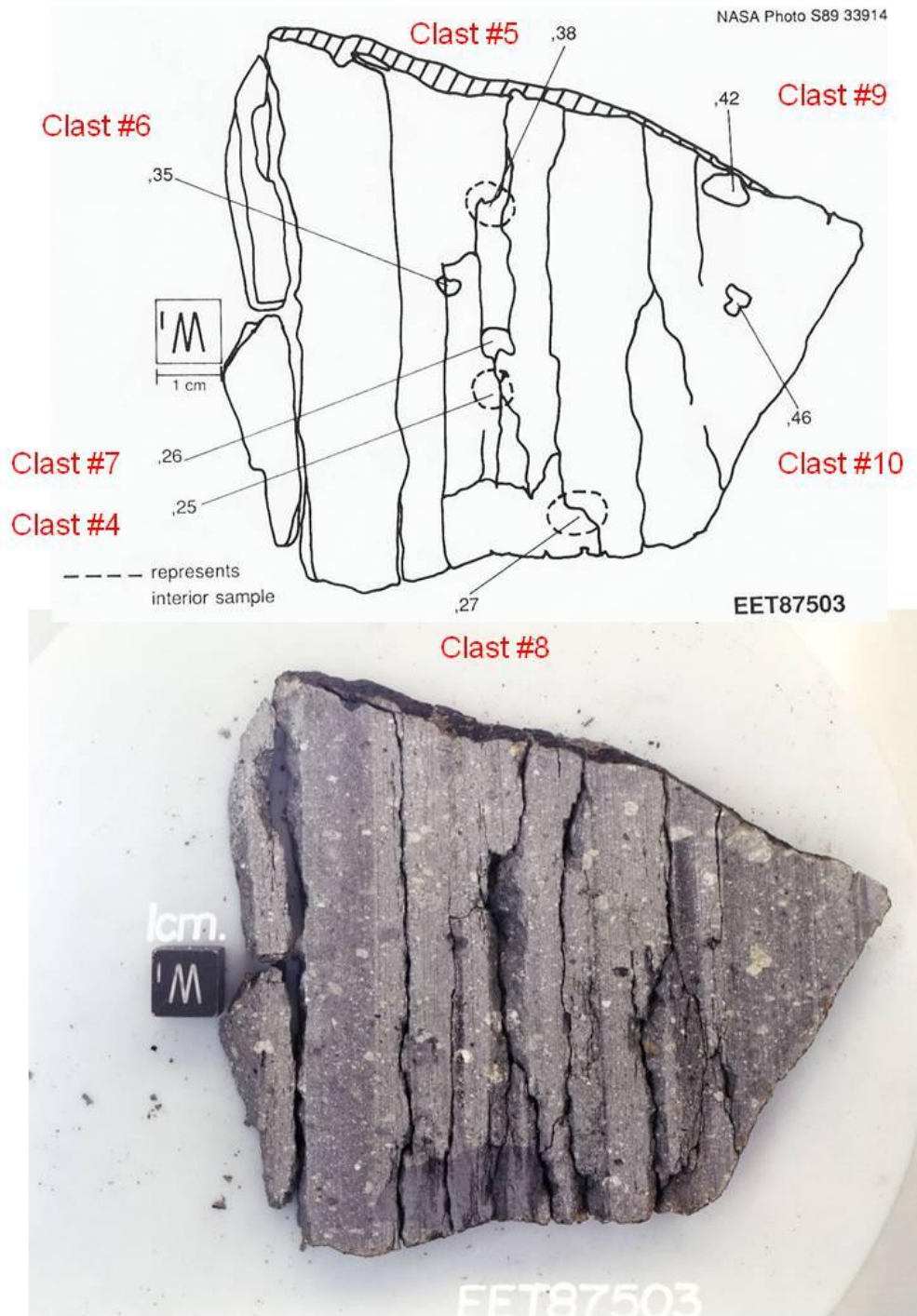


Figure 44: Locations of clasts #4 through #10 exposed in W side of slab of EET 87503 (,19). These clasts are splits ,25, 38, 35, 26, 27, 42, and 46, respectively.